

**Ecohydrodynamic model
of the Baltic Sea. Part 1.
Description of the
ProDeMo model***

OCEANOLOGIA, 47 (4), 2005.
pp. 477–516.

© 2005, by Institute of
Oceanology PAS.

KEYWORDS

Baltic Sea
Ecohydrodynamic modelling
Biogeochemical processes
Nutrients

BOGDAN OŁDAKOWSKI
MAREK KOWALEWSKI
JAN JĘDRASIK
MARIA SZYMELFENIG

Institute of Oceanography,
University of Gdańsk,
al. Marszałka Piłsudskiego 46, PL-81-378 Gdynia, Poland;
e-mail: ocemk@univ.gda.pl

Received 21 February 2005, revised 10 October 2005, accepted 20 October 2005.

Abstract

The ProDeMo (Production and Destruction of Organic Matter Model), a 3D coupled hydrodynamic-ecological model, was formulated and applied to the whole Baltic Sea and the subregion of the Gulf of Gdańsk. It describes nutrient cycles (phosphorus, nitrogen, silicon) through the food web with 15 state variables, oxygen conditions and the parameterisation of water-sediment interactions. The present version of the model takes two groups of phytoplankton – diatoms and non-diatoms – as well as zooplankton into consideration. It covers the flow of matter and energy in the sea, including river discharges and atmospheric deposition. Numerical applications are embedded on a 1 NM grid for the Gulf of Gdańsk and a 5 NM grid for the Baltic Sea.

Since the model results largely concur with observations, the model can be regarded as a reliable tool for analysing the behaviour of the Baltic ecosystem.

* This research was supported by the State Committee for Scientific Research, Poland (grant No 6 P04G 061 17). Editing assistance of the article was provided by BALTDER (EVK3-CT-2002-80005), funded by the European Commission under the 5th Framework Programme.

Some examples of the spatial-temporal variability of the most important biological and chemical parameters are presented. The model results are compared with those of other modelling research in the Baltic Sea.

Both the ProDeMo model algorithm and its computing procedures need to be further developed. The next version should therefore enable more phytoplankton groups to be defined, for example cyanobacteria, which are able to take up molecular nitrogen from the atmosphere (nitrogen fixation). Additionally, the sediment phase should be divided into active and non-active layers.

1. Introduction

Mathematical modelling is a research method enabling processes taking place in the natural environment to be analysed quantitatively and qualitatively. Mathematical models of ecosystems can also be used as tools for forecasting and evaluating the influence of human activities, or for analysing future changes to an ecosystem that may take place under the influence of external factors (Gordon et al. 1995).

Many pioneering works on modelling the North Sea ecosystem were written in the 1990s (Baretta et al. 1988, 1995, Fransz et al. 1991, Blackford & Radford 1995, Radach & Lenhart 1995, Varela et al. 1995, Moll 1997, 1998, Delhez 1998, Hoch & Garreau 1998). Fransz et al. (1991) reviewed the models applied in the research into this region. The ERSEM model presented in one of the key works (Baretta et al. 1995) described the dynamics of the seasonal variation of organisms at various trophic levels of the food chain from bacteria to fish and the related circulation of nutrients.

The Baltic Sea, a region particularly endangered by eutrophication, has also been the subject of much research in the field of ecosystem modelling (Elken 1996 (ed.), Fennel & Neumann 1996, Savchuk & Wulff 1996, Suursaar & Astok 1996 (eds.), Tamsalu 1996 (ed.), Jędrasik 1997, Ołdakowski & Renk 1997, Szymelfenig 1997 (ed.), Marmefelt et al. 2000, Fennel et al. 2001). There are even earlier papers describing particular aspects of this ecosystem and applying ecological modelling, e.g. to nitrogen cycles and oxygen conditions in the Baltic Proper (Stigebrandt & Wulff 1987). Savchuk & Wulff (1993) developed a model describing interactions between auto- and heterotrophs in the pelagic zone. Semovski & Woźniak (1995) assimilated satellite data from the North Atlantic and the Baltic Sea for an ecological model, and Semovski et al. (1996) did some similar work on the phytoplankton bloom in the Gulf of Gdańsk. Van der Vat (1994) adapted the DELWAQ model adapted for the Gulf of Gdańsk. Witek et al. (1993) compared observation data from the same basin with a simulation of the Sjöberg model, demonstrating the impact of water temperature on the rate of primary production and zooplankton decay.

The aim of this paper is to present the ProDeMo model, which describes the dynamics of production and destruction of organic matter. The ProDeMo model is a development of previous attempts at modelling this ecosystem (Ołdakowski et al. 1994, Ołdakowski & Renk 1997). The present version adopts the classic functional-group approach and parameterises basic water-sediment interactions such as the mineralisation of nutrients and their fluxes to the aqueous phase. The model's open structure allows for the addition of further functional groups (e.g. fish) or for their division into subgroups. The paper includes a detailed description of the algorithm, the whole application procedure, as well as some of results obtained when the model was applied to the Baltic Sea. This model was put through the various stages of the modelling procedure: calibration, verification and validation. The results of the validation are presented in the second part of this paper (Jędrasik & Szymelfenig 2005, this volume). The set of calibration coefficients used for solving the equations describing biogeochemical processes was obtained by comparing the simulations of the relevant state parameters with observations made in 1994–96. The simulations carried out for 1994–96 confirmed the stability of the model in a perennial cycle. The model was then applied to another three-year period, from 1998 to 2000. Since the model results largely concur with observations, the model can be regarded as a reliable tool for predicting the behaviour of the Baltic ecosystem. The paper also presents examples of the spatial-temporal variability of the most important biological and chemical parameters.

2. Description of the model

2.1. ProDeMo model

The mathematical model of the production and destruction of organic matter (ProDeMo) describes basic biogeochemical processes taking place in the marine environment. The model includes 15 state variables (Table 1), which can be divided into functional groups: phytoplankton, zooplankton, nutrients, detritus, dissolved oxygen and nitrogen, phosphorus and silicon compounds in the sediment (Fig. 1). The phytoplankton includes autotrophic organisms divided into two groups: diatoms (DIAT), and other groups of phytoplankton, i.e. non-diatoms (nDIAT). Zooplankton is restricted to organisms grazing on phytoplankton. Detritus includes all dead matter (dead phytoplankton and zooplankton; faeces), which undergoes mineralisation. Inorganic forms of nutrients include nitrate nitrogen (N-NO_3), ammonium nitrogen (N-NH_4), phosphate phosphorus (P-PO_4) and silicate silicon (Si-SiO_4). Inorganic forms of carbon were not included

Table 1. State variables of the ProDeMo Model

| State variable | Description | Unit |
|--------------------|---|--------------------|
| C_{DIAT} | Carbon in diatoms | gC m^{-3} |
| C_{nDIAT} | Carbon in other groups of phytoplankton | gC m^{-3} |
| C_{ZOO} | Carbon in the zooplankton biomass | gC m^{-3} |
| C_{DETR} | Carbon in detritus | gC m^{-3} |
| $N\text{-NO}_3$ | Nitrate nitrogen | g m^{-3} |
| $N\text{-NH}_4$ | Ammonium nitrogen | g m^{-3} |
| N_{DETR} | Nitrogen in detritus | g m^{-3} |
| $P\text{-PO}_4$ | Phosphate phosphorus | g m^{-3} |
| P_{DETR} | Phosphorus in detritus | g m^{-3} |
| Si-SiO_4 | Silicate silicon | g m^{-3} |
| Si_{DETR} | Silicon in detritus | g m^{-3} |
| DO | Dissolved oxygen | g m^{-3} |
| N_{SED} | Nitrogen in the sediment | g m^{-2} |
| P_{SED} | Phosphorus in the sediment | g m^{-2} |
| Si_{SED} | Silicon in the sediment | g m^{-2} |

in the ProDeMo model's structure because they do not limit phytoplankton growth. This is also why the ProDeMo model takes into consideration only the part of the carbon cycle that includes phytoplankton, zoological plankton and detritus. The nitrogen, phosphorus and silicon cycles are closed with regard to exchange with the bottom sediments and atmosphere. The same applies to dissolved oxygen (O_2), where the mass balance equation covers processes taking place in the water column, and also the consumption of oxygen for the mineralisation of compounds contained in the bottom sediment and for exchange through the sea surface.

The processes affecting the concentrations of particular state variables are given by the parameters in the relevant mathematical formulae – the set of equations containing 96 coefficients, whose values were established during the course of calibration (Appendix 1).

Balance equations for the phytoplankton biomass cover the following processes: phytoplankton growth (in relation to temperature, light and nutrient content), respiration, grazing by zooplankton, mortality and sinking. In the case of zooplankton, the processes of assimilation, respiration, excretion and natural mortality are taken into consideration. Besides the flow of nutrients (N, P and Si) through living organisms, the model allows for their uptake by phytoplankton and their mineralisation. Additionally, nitrification and denitrification are taken into account in the nitrogen cycle, as are the adsorption and desorption of phosphate on suspended matter in the phosphorus cycle. Detritus includes four state

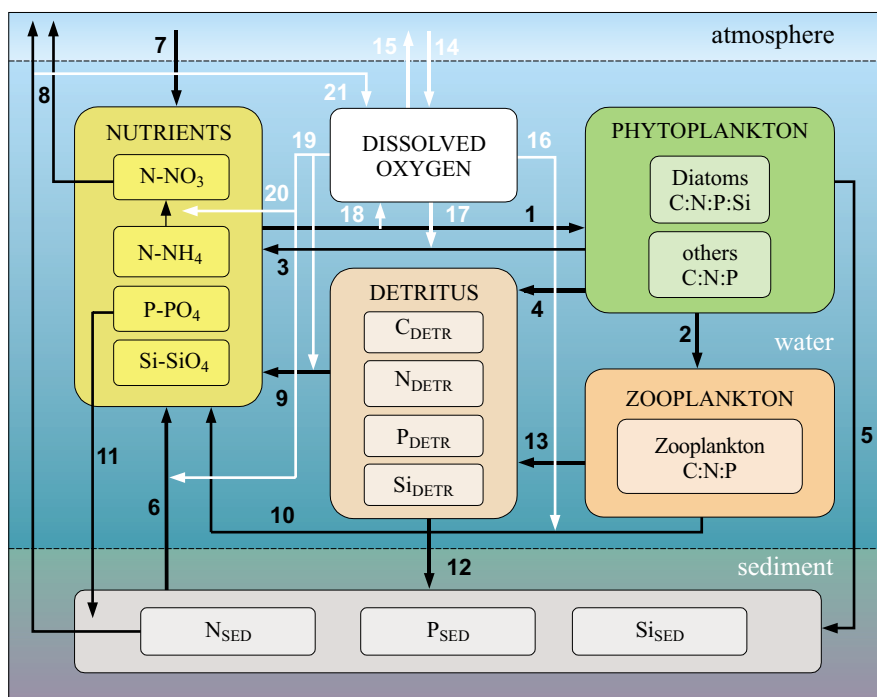


Fig. 1. State variables and processes included in the ProDeMo model: nutrient uptake (1), grazing (2), phytoplankton respiration (3), decay (4), sedimentation (5), release from sediment (6), atmospheric deposition (7), denitrification (8), mineralization (9), zooplankton respiration (10), sedimentation of phosphorus adsorbed on particles (11), sedimentation (12), zooplankton decay (13), reaeration, (14), oxygen flux to atmosphere (15), zooplankton respiration (16), phytoplankton respiration (17), assimilation (18), mineralization (19), nitrification (20), denitrification (21)

variables describing the concentrations of nitrogen, phosphorus, silicon and carbon. Processes like phytoplankton and zooplankton decay, excretion by zooplankton, mineralisation and sedimentation are taken into account for all variables. The oxygen balance includes re-aeration, photosynthesis, respiration in phytoplankton and zooplankton, mineralisation, nitrification and denitrification. The ProDeMo model also describes the penetration of sunlight into the sea water in relation to phytoplankton and detritus concentrations. The full set of mathematical formulae describing all the processes under consideration is given in Appendix 2.

2.2. Integration with the hydrodynamic model

The mathematical definition of biogeochemical processes taking place in the sea allows the ecological and hydrodynamic models to be coupled

in order to include diffusion and advection (Vested et al. 1996). The ProDeMo ecological model was thus combined with a three-dimensional hydrodynamic model of the Baltic Sea. This latter model is based on the Princeton Ocean Model (POM) (Blumberg & Mellor 1987); in order to adapt it to Baltic conditions, the numerical scheme for the computation of advection had to be modified (Kowalewski 1997). The coupling of the two models was effected by solving the advection-diffusion equation in the Cartesian coordinate system (x, y, z) for an arbitrary state variable (C_i) :

$$\begin{aligned} & \frac{\partial C_i}{\partial t} + \frac{\partial uC_i}{\partial x} + \frac{\partial vC_i}{\partial y} + \frac{\partial wC_i}{\partial z} = \\ & = \frac{\partial}{\partial x} \left(K_H \frac{\partial C_i}{\partial x} \right) + \frac{\partial}{\partial y} \left(K_H \frac{\partial C_i}{\partial y} \right) + \frac{\partial}{\partial z} \left(K_Z \frac{\partial C_i}{\partial z} \right) + \left(\frac{\partial C_i}{\partial t} \right)_{ECO}. \end{aligned} \quad (1)$$

The velocity components of flow u, v, w and the coefficients of the horizontal and vertical diffusion of mass K_H and K_Z were calculated in the hydrodynamic model. Biogeochemical processes, which cause the concentrations of particular state variables (C_i) to change, are represented by the last term in eq. (1). The solution of eq. (1) allows a local change in concentration C_i to be determined in time with respect to diffusion and advection as well as the biological and chemical processes taking place in the water column.

The sigma transformation was applied to the model, making it possible to divide the vertical profile at each point in the sea, irrespective of its depth, into an equal number of layers (Fig. 2). Eq. (1) was converted from the Cartesian coordinate system (x, y, z) to the σ -system (x, y, σ) :

$$\begin{aligned} & \frac{\partial DC_i}{\partial t} + \frac{\partial DuC_i}{\partial x} + \frac{\partial DvC_i}{\partial y} + \frac{\partial D\omega C_i}{\partial \sigma} = \\ & = \frac{\partial}{\partial x} \left(HK_H \frac{\partial C_i}{\partial x} \right) + \frac{\partial}{\partial y} \left(HK_H \frac{\partial C_i}{\partial y} \right) + \frac{\partial}{\partial \sigma} \left(\frac{K_Z}{D} \frac{\partial C_i}{\partial \sigma} \right) + \left(\frac{\partial DC_i}{\partial t} \right)_{ECO}; \end{aligned} \quad (2)$$

where $D = H + \eta$; η – free surface elevation, H – sea depth, ω – vertical velocity in the new coordinate system defined as the velocity normal to the sigma surface:

$$\omega = w + u \left(\sigma \frac{\partial D}{\partial x} + \frac{\partial \eta}{\partial x} \right) + v \left(\sigma \frac{\partial D}{\partial y} + \frac{\partial \eta}{\partial y} \right) + \sigma \frac{\partial D}{\partial t} + \frac{\partial \eta}{\partial t}. \quad (3)$$

The use of the sigma transformation enabled better mapping of the bottom boundary layer, and made for a simplified numerical calculation scheme. On the other hand, particular layers do not lie exactly horizontally, and this causes horizontal diffusion and inaccuracies in calculating horizontal pressure gradients (Haney 1991), which may in turn result in calculation errors. In order to minimise this type of error, a special technique was

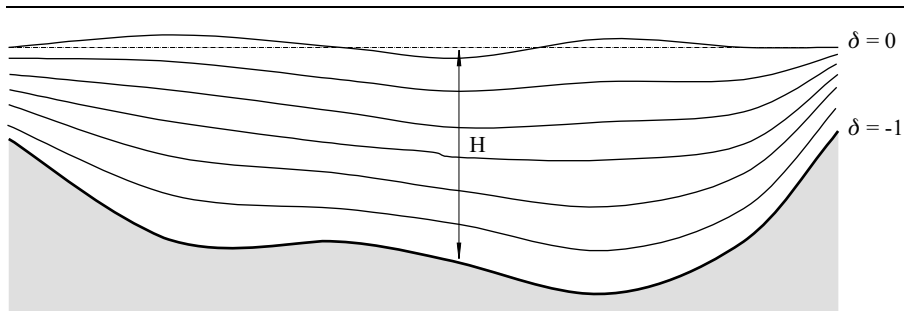


Fig. 2. Sigma transformation concept

applied, consisting in subtracting the area-averaged climatic value before calculating the horizontal gradient of a given parameter (Gary 1973, Mellor et al. 1994). This method has a relaxation character, i.e. in the case where no other factors are present, the three-dimensional fields of state variables will approach their climatic distribution after a long period of simulation. The water column was divided into 18 layers of unequal thickness; layers of smaller thickness were adopted in order to produce a better map of the surface and bottom boundary layer.

The model calculations cover the whole Baltic Sea with the sub-region of the Gulf of Gdańsk. The open boundary was located between the Kattegat and Skagerrak, where water exchange with the North Sea takes place. A radiation boundary condition was applied to vertically averaged flows with the assumption of a constant sea level in the Skagerrak. If the instantaneous value of the free surface elevation is larger than the adopted constant value, the outflow of water from the Baltic occurs in proportion to the difference in these values. In the contrary case, when the sea level in the Kattegatt is lower, water flows in from the Skagerrak. At the open boundary, the condition of salinity was assumed constant in time, which means that the vertical salinity distribution in the water flowing from the North Sea to the Baltic is constant. However, the salinity of the waters flowing out of the Baltic is time-variable, i.e. the assumed salinity is calculated in the grid points adjacent to the open boundary. For modelling the temperature and all the state variables, the horizontal gradient in the normal direction of the border was assumed equal to zero as a coastal condition on the open boundary. This means that both the water flowing out of the calculation area and the water flowing into it have the same temperature or state variable value, which was calculated as a result of the model simulation near the open boundary.

The model includes two areas with different spatial grid resolutions: the Baltic (5 NM) and the Gulf of Gdańsk (1 NM) (Fig. 3). Twenty- and four-minute time steps were used for the Baltic Sea and the Gulf of

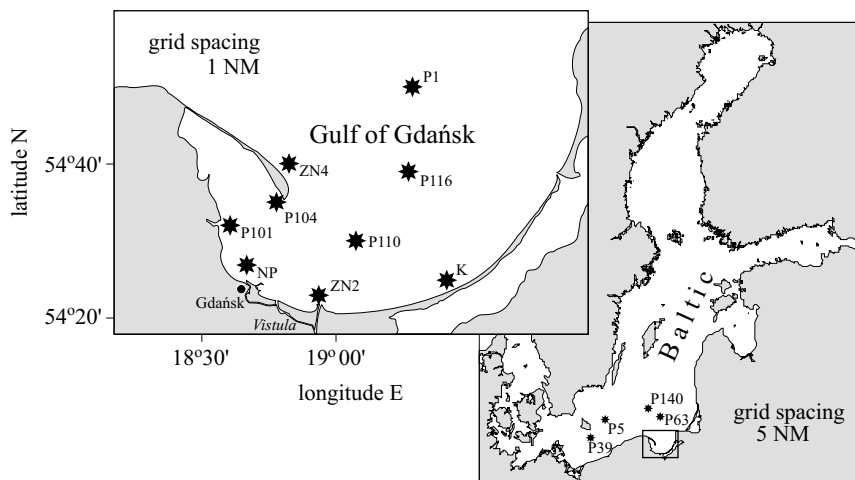


Fig. 3. Modelled areas (the Baltic and the Gulf of Gdańsk) with monitoring stations

Gdańsk respectively. Calculations in those two areas were simultaneous and information at the boundary between them was exchanged after every time step (20 minutes). All the model variables calculated at the border of one area served as a boundary condition for the other area. The algorithm, which enables this connection to be made, ensures the conservation of mass and energy.

2.3. Data used for model simulations

Carried out for the periods 1994–96 and 1998–2000, the model simulations took discharges and loads from 125 rivers flowing into the Baltic Sea into account. For the River Vistula daily discharge and temperature readings were considered along with the concentrations of nitrates, ammonia, phosphorus, total nitrogen, total phosphorus and dissolved oxygen measured twice a week (daily values interpolated). For the other rivers the water discharges and temperatures for each day of the year were calculated from trigonometric series describing the seasonal variation in river outflow established on the basis of data gathered over several decades (Cyberski 1997). Nutrient concentrations and dissolved oxygen were assumed stable on the basis of the available data (Stålnacke 1996). The influx of nitrogen and phosphorus compounds from the atmosphere was taken from Falkowska (1985).

The solar energy input was calculated for each time step on the basis of astronomical data (solar altitude) and meteorological conditions (Krężel 1997). The other components of the heat balance at the sea surface were

given by parameters (Jędrasik 1997) calculated from meteorological data and simulated sea-surface temperatures. The meteorological data – wind field, air temperature, atmospheric pressure, vapour pressure – were taken from the UMPL mesoscale operational weather model (Herman-Iżycki et al. 2002). The initial conditions for the temperature, salinity and nutrient fields were adopted on the basis of their climatic distributions in the Baltic Sea in January. Once the model was started, the changes in temperature and salinity distributions were forced only by time-variable weather conditions and river inflows. No recorded hydrological data was assimilated.

2.4. Calibration of the model

The calibration was based on a comparison of the simulation results with the relevant environmental data from 1994–96 (weather, hydrological, terrestrial and atmospheric discharge of nutrients). The values of the coefficients adopted were such as to render the simulations as similar as possible to the observed seasonal distribution of nutrients, the annual cycle of primary production, and the annual variation in phytoplankton and zooplankton.

The calibration process was divided into two stages: the first was based on one-dimensional hydrodynamic and biogeochemical models (1D), which enabled calculations to be performed promptly, the second on a three-dimensional model (3D), which required 60-hour calculations to simulate a three-year period. Measurement data made available by the IMWM in Gdynia were used for this purpose. Station P1 in the Gdańsk Deep was the principal measuring station in the first stage of calibration, while monitoring stations P101, P104, P110, P116, ZN2, ZN4, NP, K in the Gulf of Gdańsk, P140, P63 in the open waters of the Gdańsk Basin, and P5 in the Bornholm Basin (Fig. 3) were used for the validation.

The parameters adopted for the comparisons were the concentrations of nitrate nitrogen (N-N₀₃), ammonium nitrogen (N-NH₄), total nitrogen (N-Tot), phosphate phosphorus (P-PO₄), total phosphorus (P-Tot), dissolved oxygen (O₂), silicate silicon (Si-SiO₄) and the water temperature measured at the standard depths (2.5 m, 7.5 m, 10 m, 15 m, 20 m, 30 m, 40 m, 50 m, 60 m, 70 m, 80 m, 90m, 100m) at monthly intervals during 1994–96.

The first calibration stage based on the 1D model enabled its sensitivity to be analysed. The changes in the minimum and optimum light intensities and temperatures affected the time of appearance and intensity of the phytoplankton bloom, the rate of nutrient depletion, and the phytoplankton biomass. The principal coefficients obtained as a result of this calibration were changed after advection, horizontal diffusion and river inflow were

taken into account. Finally, a table of coefficients was obtained (Appendix 1) to complete the equations describing biogeochemical processes in southern Baltic waters (Appendix 2).

2.5. Comparison of model results with measurements

The modelled values were compared with those measured at the standard depths at selected observation stations (Fig. 2). The seasonal vertical distribution of calculated and measured parameters in 1995 was analysed for station P1 (Fig. 4). In the surface layer, the modelled nitrate concentrations were in accordance with the measurements. Summer measurements indicated, however, that nitrate was fully depleted down to

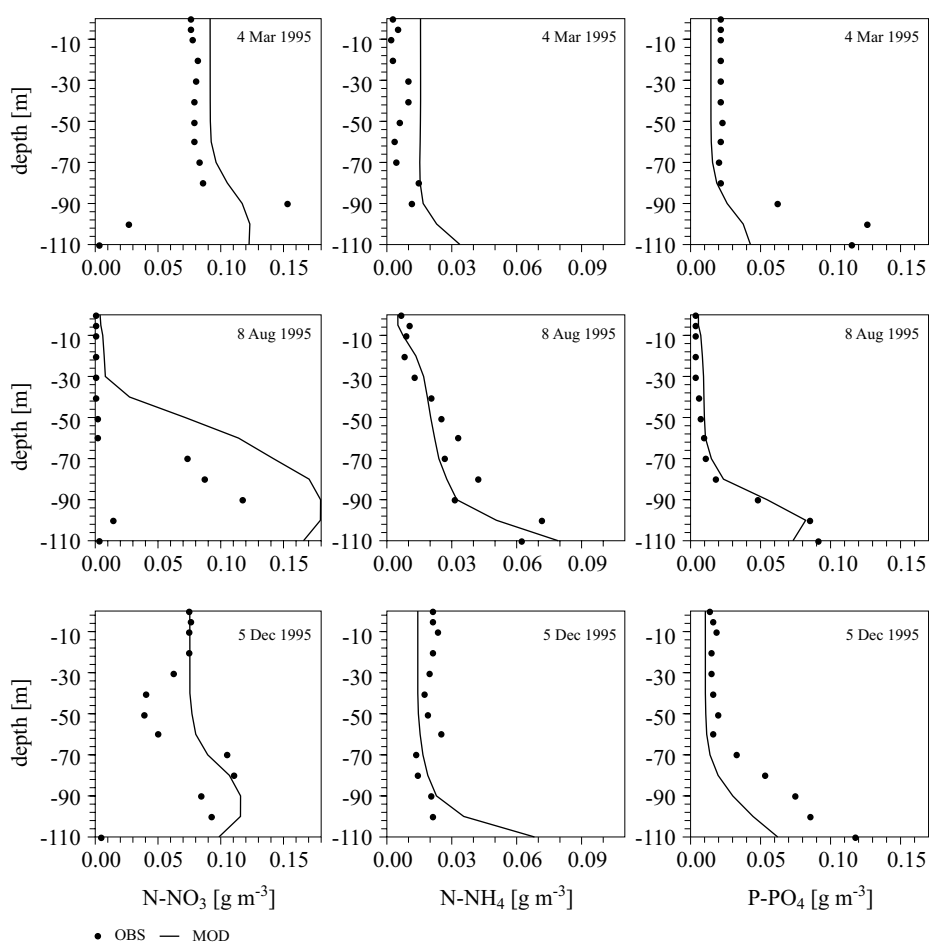


Fig. 4. Seasonal variability in 1995 of the observed vertical distributions (OBS) and the modelled (MOD) parameters: nitrate nitrogen, ammonium nitrogen and phosphate phosphorus in the Gdańsk Deep at station P1

60 metres, but according to the model, only down to 30 metres. Moreover, the modelled distribution of nitrates in the near-bottom layer did not agree with observations. The calculated distribution of ammonium nitrogen concentrations in the different seasons of 1995 conformed to the measured values. Phosphate phosphorus concentrations reached values approaching those measured during the spring and the summer down to 80 metres, and during late autumn down to 60 metres (Fig. 4). The same applied to silicate silicon and dissolved oxygen (not shown). In the bottom layer beneath the halocline, the calculated concentrations of silicates and phosphates were underestimated, while dissolved oxygen was overestimated in relation to the measurements. The modelled vertical water temperature distributions were consistent with observations (not shown).

Apart from their variability in selected periods at standard depths, the model results were analysed at the water surface, in the halocline and near the bottom (Figs 5–6). Comparison of surface distributions of the above parameters at stations P1, P140 and P5 (Fig. 2) during 1994–2000 did demonstrate the recurrence of annual cycles, but no definite trend was discernible (Fig. 5). This indicates that the model is functioning properly. At each of these stations, there was a regular summer depletion of mineral nitrogen and phosphorus. Silicate silicon concentrations were lower. The variability of modelled and observed phosphate phosphorus concentrations at P140 and P5, and nitrate nitrogen at P140 were highly correlated (Fig. 5). Modelled nitrate nitrogen values in the Gdańsk and Bornholm Deeps resembled the observations, with respective correlation coefficients of 0.67 and 0.69. Silicate silicon values displayed a lower level of similarity, especially at P5 in the Bornholm Basin. The simulations of ammonium nitrogen were the weakest (Fig. 5), despite a correlation coefficient of 0.33 for the Gdańsk Deep. It is worth stressing that the values modelled for the period 1998–2000 did not deviate much from those simulated for 1994–96.

The simulations and the standard depth measurements at all the stations in the Gulf of Gdańsk in 1998–2000 (Table 2) were compared. With respect to all the parameters, the correlations of the observed regularities decreased from the surface to the bottom; the values for silicate silicon and phosphate phosphorus even dropped below zero. The correlations for the layers from the surface down to 20 m for phosphate phosphorus, to 50 m for nitrate nitrogen and to 80 m for dissolved oxygen, silicate silicon and total phosphorus were quite good (> 0.6). In spite of incompatibilities in the coastal zone and in the deep layers, the simulation results for most of the variables converge satisfactorily with observations. The consistency of the calculated values with those measured in the vertical distribution was particularly good with regard to dissolved oxygen and total phosphorus.

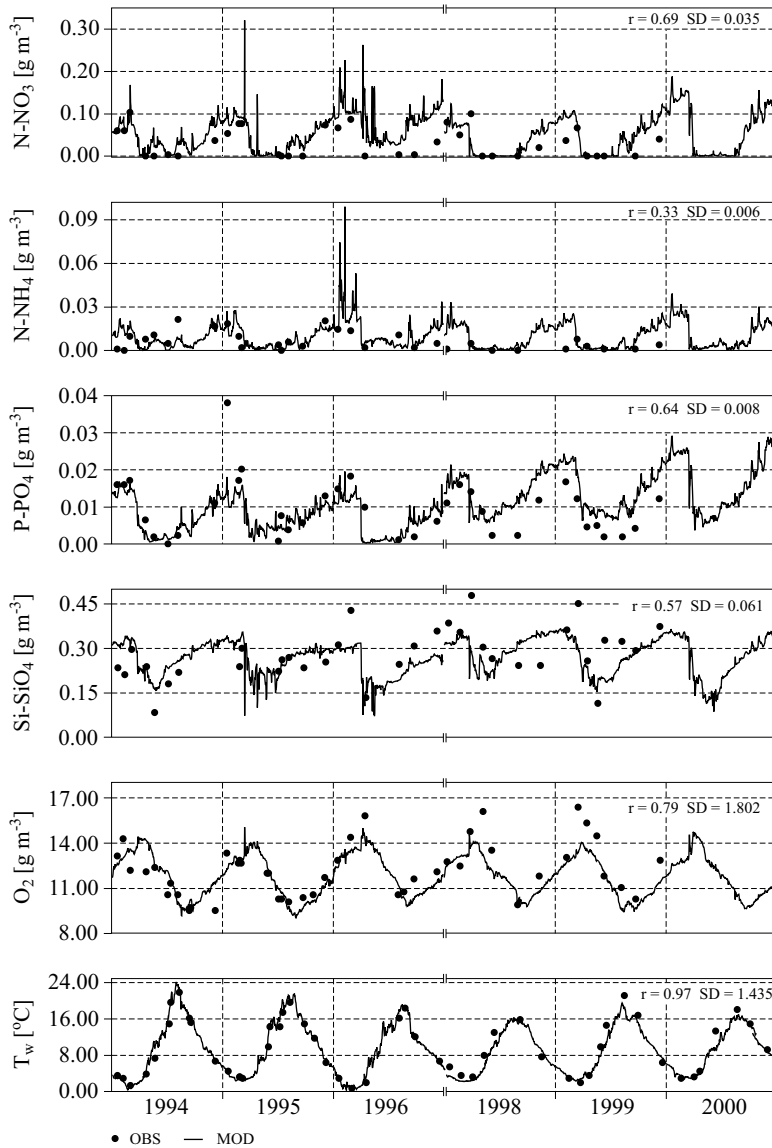


Fig. 5a. The temporal distribution (1994–2000) of the observed (OBS) and modelled (MOD) parameters: nitrate nitrogen, ammonium nitrogen, phosphate phosphorus, silicate silicon, dissolved oxygen and water temperature in the Gdańsk Deep (station P1, depth – 0 m)

The correlations calculated for all measurements for three stations representing different areas of the southern Baltic showed the results of the model calculations to be of the same quality, except for a few poorer results for nitrogen compounds at station P140 (Table 3).

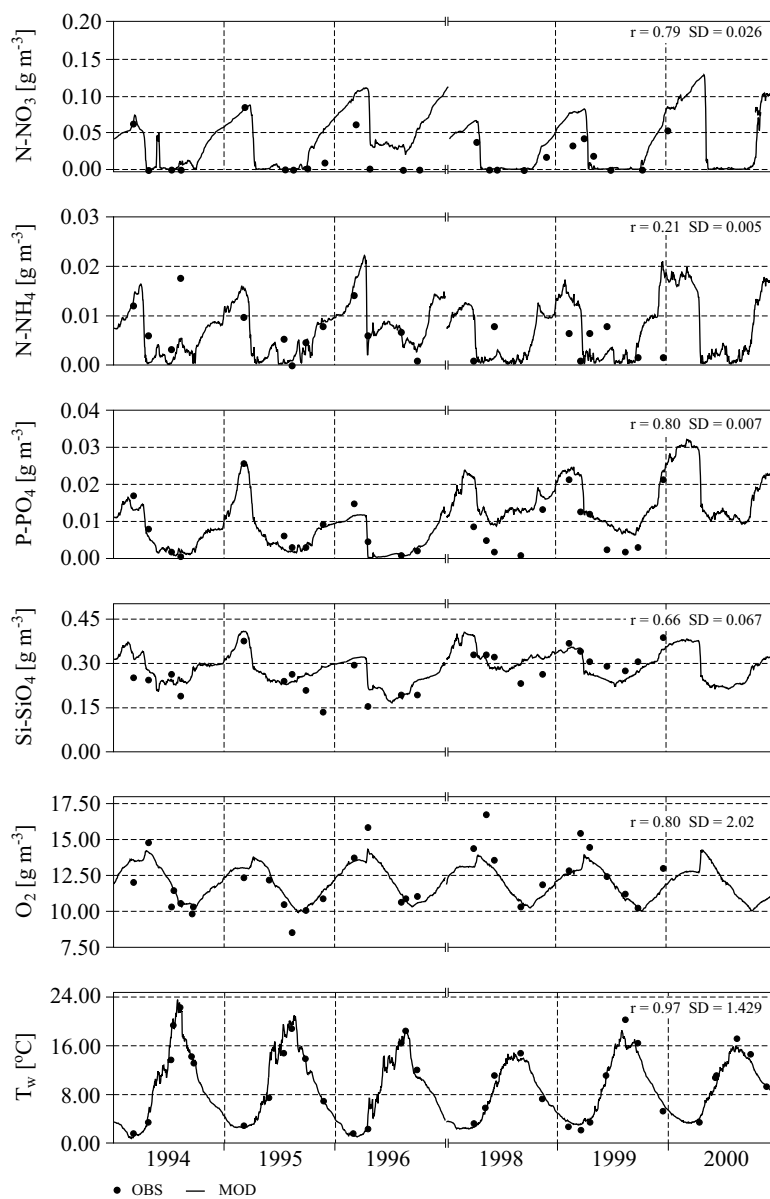


Fig. 5b. The temporal distribution (1994–2000) of the observed (OBS) and modelled (MOD) parameters: nitrate nitrogen, ammonium nitrogen, phosphate phosphorus, silicate silicon, dissolved oxygen and water temperature in the Gdańsk Deep (station P140, depth – 0 m)

The correlations for the basic variables in the 1998–2000 validation period provide evidence for the good quality of the model. The results of the correlation, a little worse for forms of nitrogen and slightly better for

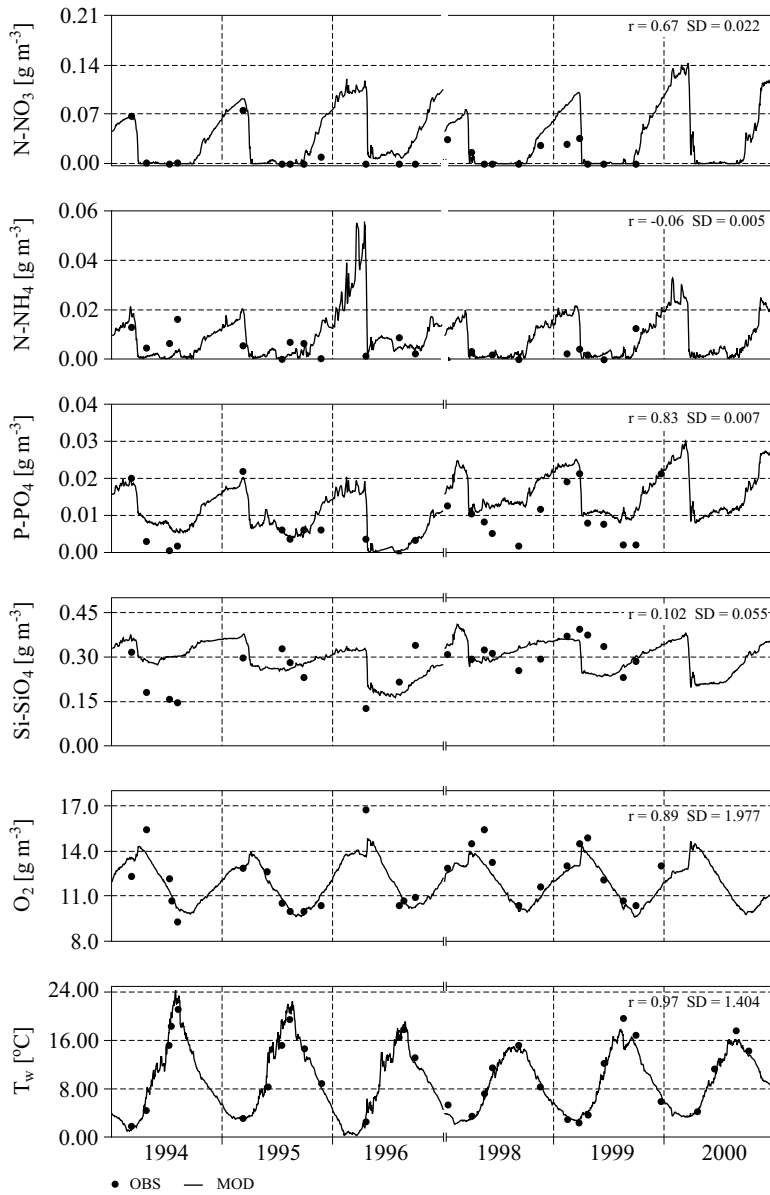


Fig. 5c. The temporal distribution (1994–2000) of the observed (OBS) and modelled (MOD) parameters: nitrate nitrogen, ammonium nitrogen, phosphate phosphorus, silicate silicon, dissolved oxygen and water temperature in the Gdańsk Deep (station P5, depth – 0 m)

phosphate phosphorus and silicate silicon, confirm the good quality of the calibration and are a favourable test for the model. This result also testifies to the fact that the environmental conditions did not change radically and

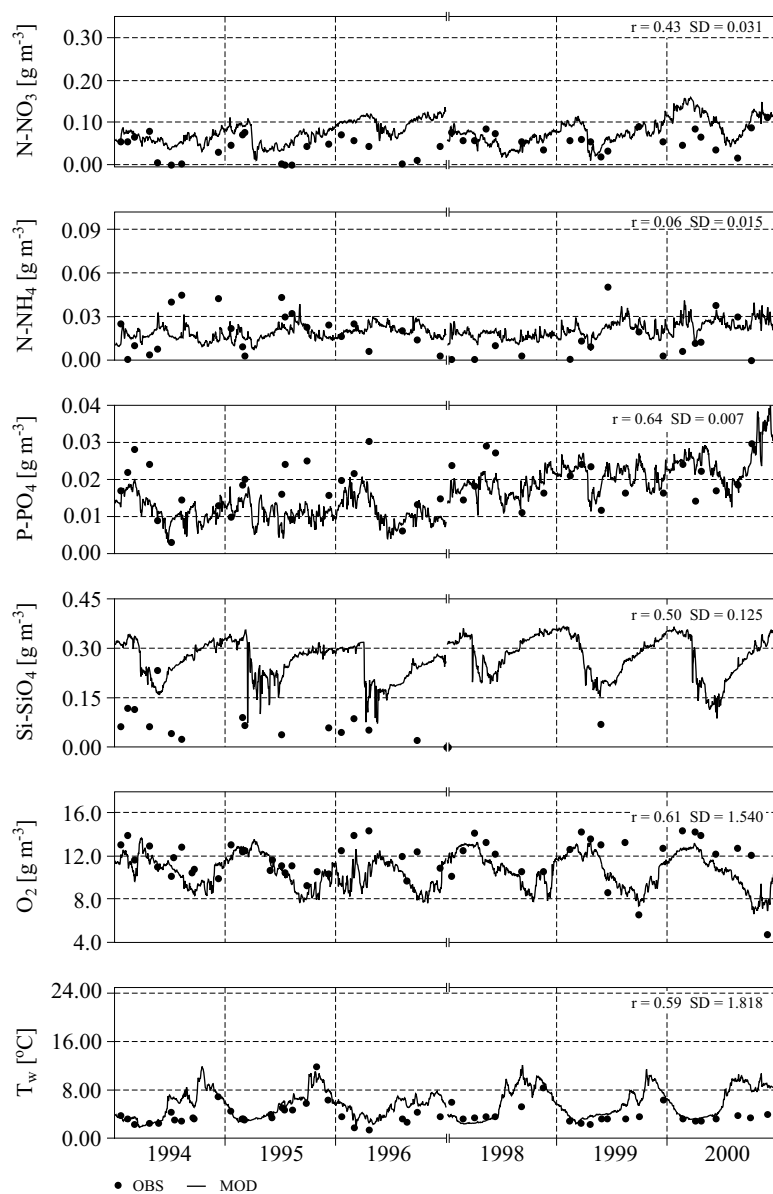


Fig. 6a. The temporal distribution (1994–2000) of the observed (OBS) and modelled (MOD) parameters: nitrate nitrogen, ammonium nitrogen, phosphate phosphorus, silicate silicon, dissolved oxygen and water temperature in the Gdańsk Deep (station P1, depth – 60 m)

that the various processes were regular. The details of the model validations and the applied statistical measures are given in Jędrasik & Szymelfenig (2005, this volume).

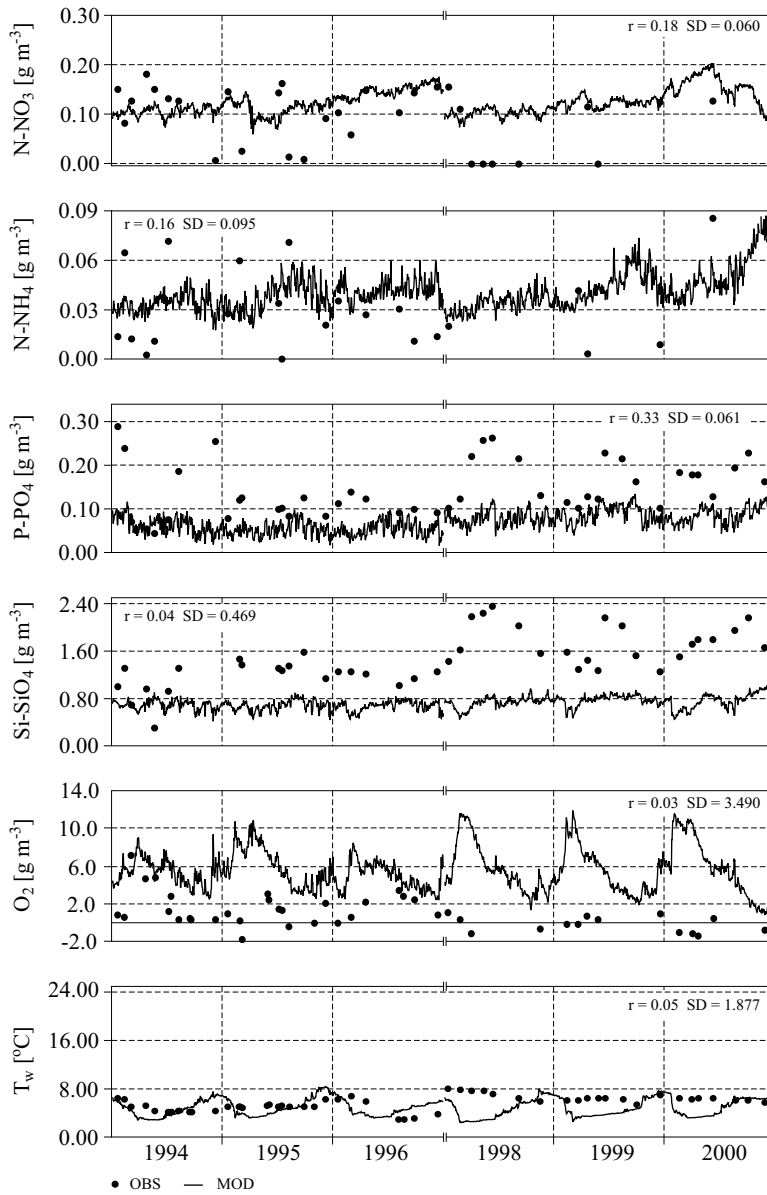


Fig. 6b. The temporal distribution (1994–2000) of the observed (OBS) and modelled (MOD) parameters: nitrate nitrogen, ammonium nitrogen, phosphate phosphorus, silicate silicon, dissolved oxygen and water temperature in the Gdańsk Deep (station P1, depth – 100 m)

3. Results of the model simulations

ProDeMo calculations for two three-year periods (1994–96 and 1998–2000) enabled the spatial distribution of physical, chemical and biological

Table 2. Correlation coefficients R and standard deviations SD of selected state variables of the ProDeMo model at observation stations in the Gulf of Gdańsk in 1998–2000

| Z [m] | NO ₃ | | NH ₄ | | N _{tot} | | PO ₄ | | P _{tot} | | Si | | O ₂ | | Number of observations |
|-------|-----------------|------|-----------------|------|------------------|------|-----------------|------|------------------|------|------|------|----------------|------|------------------------|
| | R | SD | R | SD | R | SD | R | SD | R | SD | R | SD | R | SD | |
| 0 | 0.73 | 0.02 | -0.14 | 0.01 | 0.13 | 0.07 | 0.84 | 0.01 | 0.31 | 0.01 | 0.4 | 0.05 | 0.88 | 0.83 | 57 |
| 10 | 0.66 | 0.02 | -0.07 | 0.01 | 0.02 | 0.08 | 0.81 | 0.01 | 0.13 | 0.01 | 0.32 | 0.07 | 0.88 | 0.9 | 57 |
| 20 | 0.76 | 0.02 | -0.16 | 0.01 | 0.11 | 0.05 | 0.75 | 0.01 | 0.12 | 0.01 | 0.33 | 0.06 | 0.87 | 0.95 | 57 |
| 30 | 0.72 | 0.02 | 0.15 | 0.01 | 0.09 | 0.03 | 0.55 | 0.01 | 0.07 | 0.01 | 0.03 | 0.07 | 0.65 | 1.22 | 57 |
| 40 | 0.66 | 0.04 | 0.27 | 0.01 | 0.07 | 0.04 | 0.61 | 0.01 | 0.01 | 0.01 | 0.02 | 0.06 | 0.72 | 1.16 | 57 |
| 50 | 0.3 | 0.03 | 0.35 | 0.01 | 0.01 | 0.04 | 0.45 | 0.01 | 0.18 | 0.01 | 0.27 | 0.09 | 0.72 | 1.36 | 57 |
| 60 | 0.18 | 0.03 | 0.27 | 0.01 | 0.15 | 0.04 | 0.57 | 0.01 | 0.4 | 0.01 | 0.47 | 0.18 | 0.87 | 1.55 | 57 |
| 70 | 0.05 | 0.04 | 0.37 | 0.01 | 0.13 | 0.03 | 0.55 | 0.04 | 0.49 | 0.04 | 0.66 | 0.38 | 0.76 | 2.13 | 57 |
| 80 | -0.12 | 0.06 | 0.46 | 0.03 | 0.13 | 0.03 | 0.47 | 0.06 | 0.47 | 0.05 | 0.49 | 0.45 | 0.71 | 2.37 | 57 |
| 90 | -0.53 | 0.05 | 0.55 | 0.04 | - | - | 0.25 | 0.04 | - | - | 0.35 | 0.38 | 0.31 | 3.75 | 57 |
| 100 | 0.25 | 0.04 | 0.25 | 0.09 | -0.06 | 0.1 | 0.27 | 0.05 | - | - | 0.13 | 0.55 | 0.36 | 4.29 | 23 |
| 110 | 0.19 | 0.04 | 0.22 | 0.09 | - | - | 0.2 | 0.05 | - | - | 0.05 | 0.51 | 0.36 | 3.71 | 23 |

Table 3. Correlation coefficients R and standard deviations SD of selected state variables of the ProDeMo model at observation stations in the southern Baltic in 1998–2000

| Station | NO ₃ | | NH ₄ | | N _{tot} | | PO ₄ | | P _{tot} | | Si | | O ₂ | | Number of observations |
|---------|-----------------|------|-----------------|------|------------------|------|-----------------|------|------------------|------|------|------|----------------|------|------------------------|
| | R | SD | R | SD | R | SD | R | SD | R | SD | R | SD | R | SD | |
| P1 | 0.52 | 0.05 | 0.68 | 0.06 | 0.16 | 0.09 | 0.88 | 0.04 | 0.82 | 0.05 | 0.89 | 0.41 | 0.83 | 4.02 | 286 |
| P140 | 0.70 | 0.04 | 0.30 | 0.01 | 0.15 | 0.08 | 0.82 | 0.02 | 0.70 | 0.03 | 0.77 | 0.24 | 0.61 | 2.16 | 198 |
| P5 | 0.69 | 0.04 | 0.50 | 0.02 | 0.12 | 0.08 | 0.82 | 0.05 | 0.78 | 0.07 | 0.86 | 0.41 | 0.96 | 1.78 | 188 |

parameters in the Baltic to be traced. The spring bloom of diatoms (DIAT) appeared earliest in the Danish Straits area, in March (Fig. 7), and in the coastal zone and the southern part of the Baltic Proper following the dependence on temperature and solar radiation. It embraced the whole of the Baltic Proper in April and appeared in the Gulf of Finland in early May. Then, too, the diatom bloom appeared in the coastal zone of the Gulf of Bothnia, and in the second half of May moved into its deeper waters. The bloom of the second group of phytoplankton (nDIAT) began in the Kattegatt and the Pomeranian Bay in late May (Fig. 8). In contrast to the diatom bloom, it then appeared very swiftly in the coastal zones of

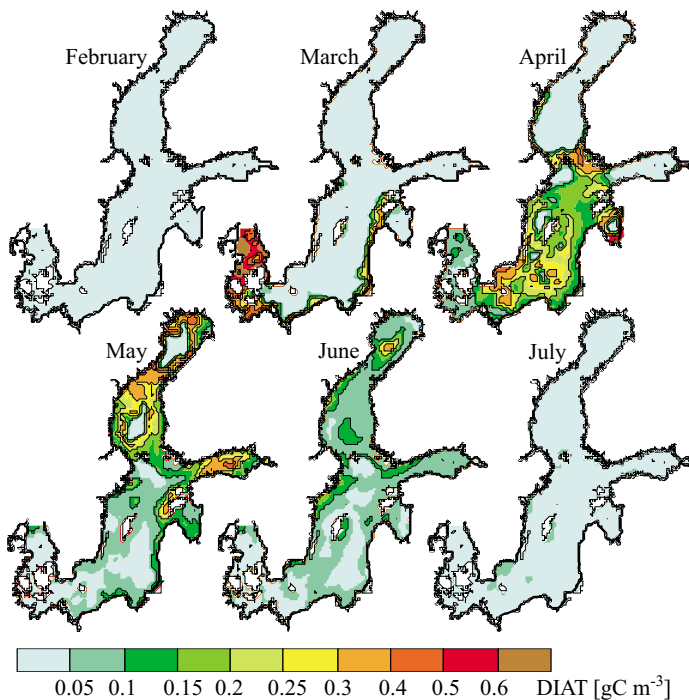


Fig. 7. Surface distribution of the diatom biomass for the year 2000

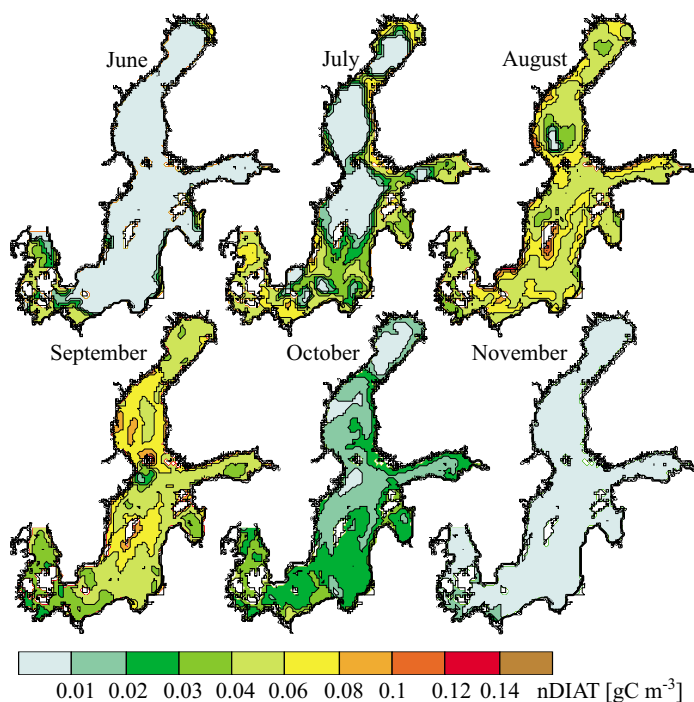


Fig. 8. Surface distribution of the non-diatom biomass for the year 2000

the entire Baltic, and by mid-June it reached the northern part of the Gulf of Bothnia, where the diatom bloom had just come to an end. As in the case of the diatom bloom, the bloom zones moved from the shallow coastal zones towards deeper waters. The influence of water temperature on the timing of the bloom is evident. Calculations for other years showed that phytoplankton growth (nDIAT) occurred later in the years when the water was cooler in July (1995, 1996, 2000). Once nDIAT had bloomed in late July–early August, the biomass concentration remained at about the same level in the whole Baltic. In September, blooms of lesser intensity appeared throughout the Baltic, but in October, only in the southern and western regions of the sea; in early November they ceased altogether (Fig. 8). Our simulation results appear to accord with the current views regarding the succession of the particular phytoplankton groups. The first one (DIAT) provides a good description of the spring diatom bloom, while the second (nDIAT) relates to the other species, namely, the green algae, blue-green algae, dinoflagellates and autumn diatoms. Analysis of the spatial distributions of the plankton biomass confirms, among other things, the well-known west-east bloom shift in the southern Baltic from shallower to deeper waters (Neumann 2000).

The distributions of zooplankton concentrations were spatially very heterogeneous (Fig. 9). Like the phytoplankton, the zooplankton biomass

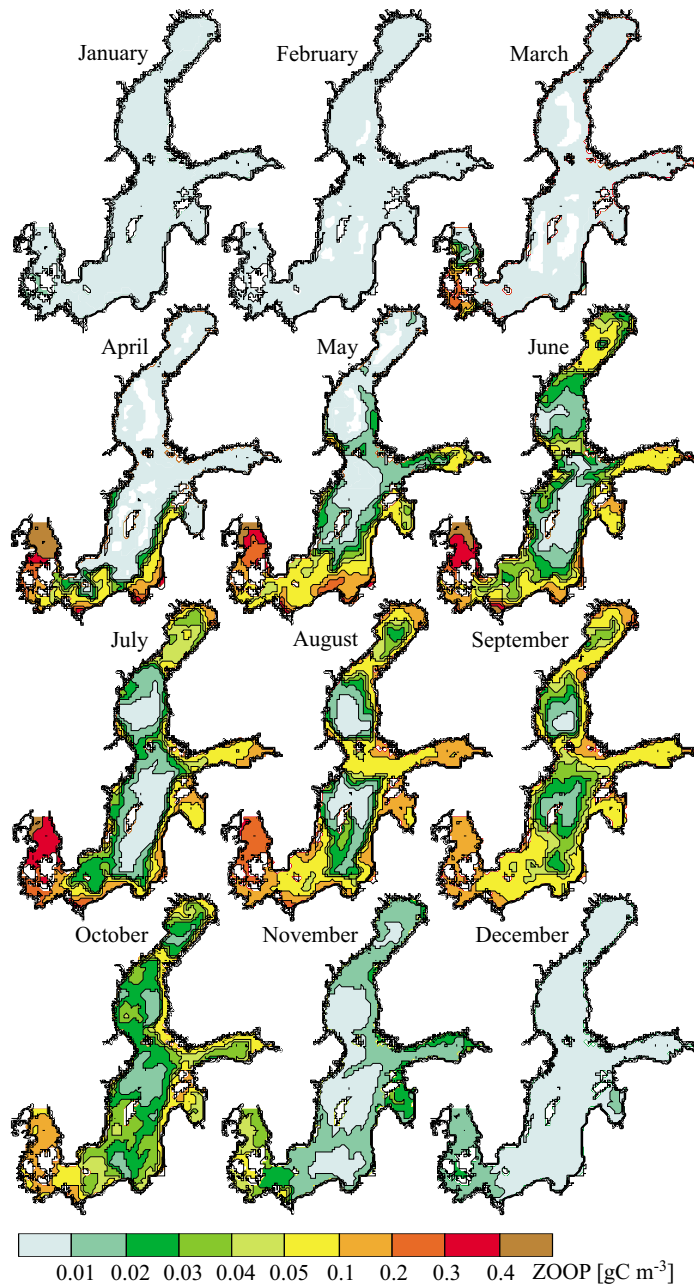


Fig. 9. Surface distribution of the zooplankton biomass for the year 2000

starts to grow in the Danish Straits, later along the southern Baltic coast, then in the Gulfs of Riga and Finland, and off the eastern shores of the Gulf of Bothnia. Throughout the summer period (June–September), concentrations of zooplankton remained quite consistently high in almost the whole Baltic; values were higher still in coastal waters. This is the result of the high dependence of zooplankton growth on food availability (high concentration of non-diatoms) and water temperature.

The seasonal variability in nitrate and ammonium concentrations (Fig. 10) in the surface layer of the Baltic seems adequately approximated by the model results. Concentrations of N-NO_3 and N-NH_4 (Figs 10 and 11) are high in the winter and early spring, especially near the mouths of rivers, where large nitrogen loads are present. The spring depletion of nitrogen compounds follows the shift in the spring diatom bloom zones. During the three-year simulations a tendency for inorganic nitrogen concentrations to increase becomes apparent, particularly in the Gulf of Riga, where nitrates are not depleted even in the summer. Nevertheless, phosphates are consumed there, which obviously limits phytoplankton growth (Fig. 12). This situation does not seem very realistic: it may be the effect of overestimating the nitrogen load or underestimating the amount of phosphorus entering the Gulf of Riga. A similar gradual increase in phosphate concentrations during the three-year simulations is seen in the Kattegatt, but here the cause may be the coastal condition adopted on the model's open border between the Kattegatt and the Skagerrak.

As far as silicates and phosphates are concerned, a rising tendency was recorded (Fig. 13). In other regions of the Baltic (e.g. in the southern part of the Gulf of Bothnia), there is an increase in inorganic silicon concentrations in the first year of the simulation, but in subsequent years of the simulation this phenomenon does not occur, so it could be a consequence of the adopted initial conditions. Silicate depletion was only sporadic, occurring over a limited area during the spring diatom bloom.

The temporal-spatial variability in dissolved oxygen (Fig. 14) concentrations is mainly the outcome of changes in water temperature (Fig. 15), as oxygen concentrations are usually close to saturation in the surface layer of the sea. In the spring, however, oxygen levels in the coastal zone are very high as a result of intensive assimilation during the phytoplankton bloom.

4. Discussion

The structure of the combined ProDeMo + 3D transport model enabled basic relationships between organic and inorganic matter to be mapped in the annual cycle. The principle that 'the simpler the model, the better' was adopted in developing the algorithm for the ProDeMo

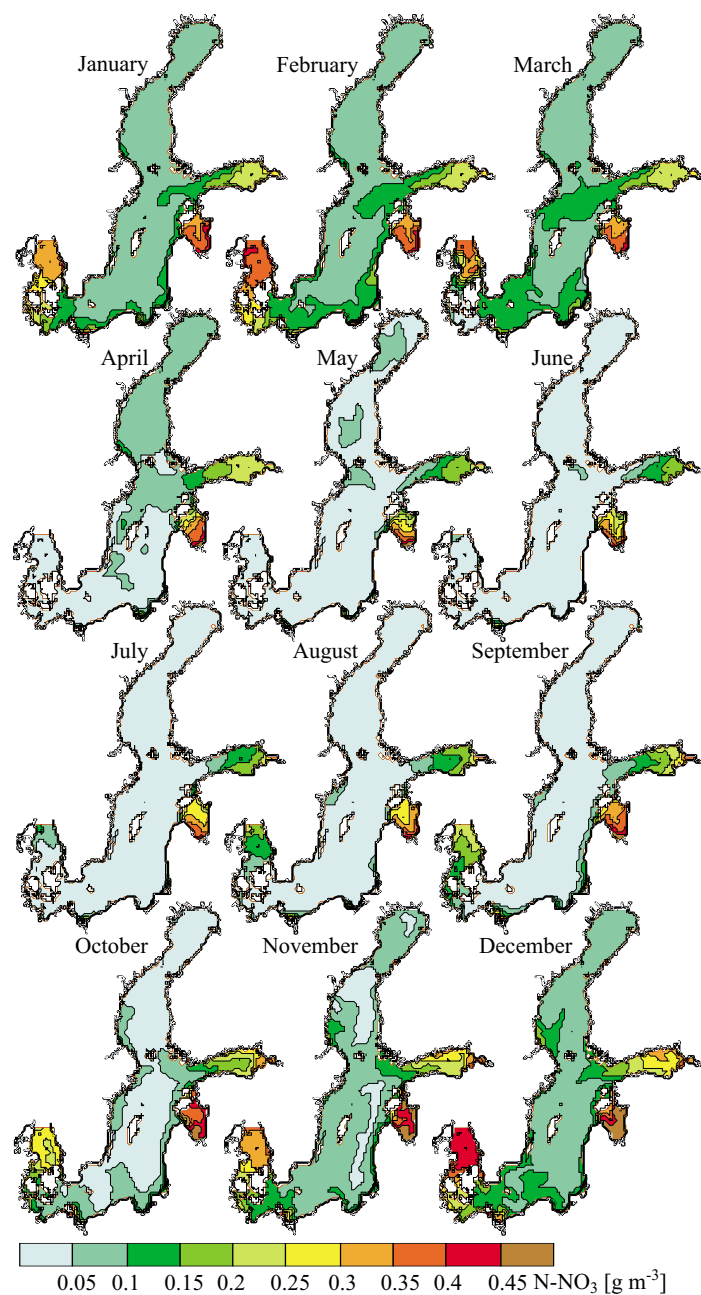


Fig. 10. Surface distribution of nitrate nitrogen for the year 2000

model (Jørgensen 1998). A development of previous versions of the ProDeMo model (Kowalewski & Jędrasik 1993, Ołdakowski et al. 1994, Ołdakowski & Renk 1997), the present version has been extended to include

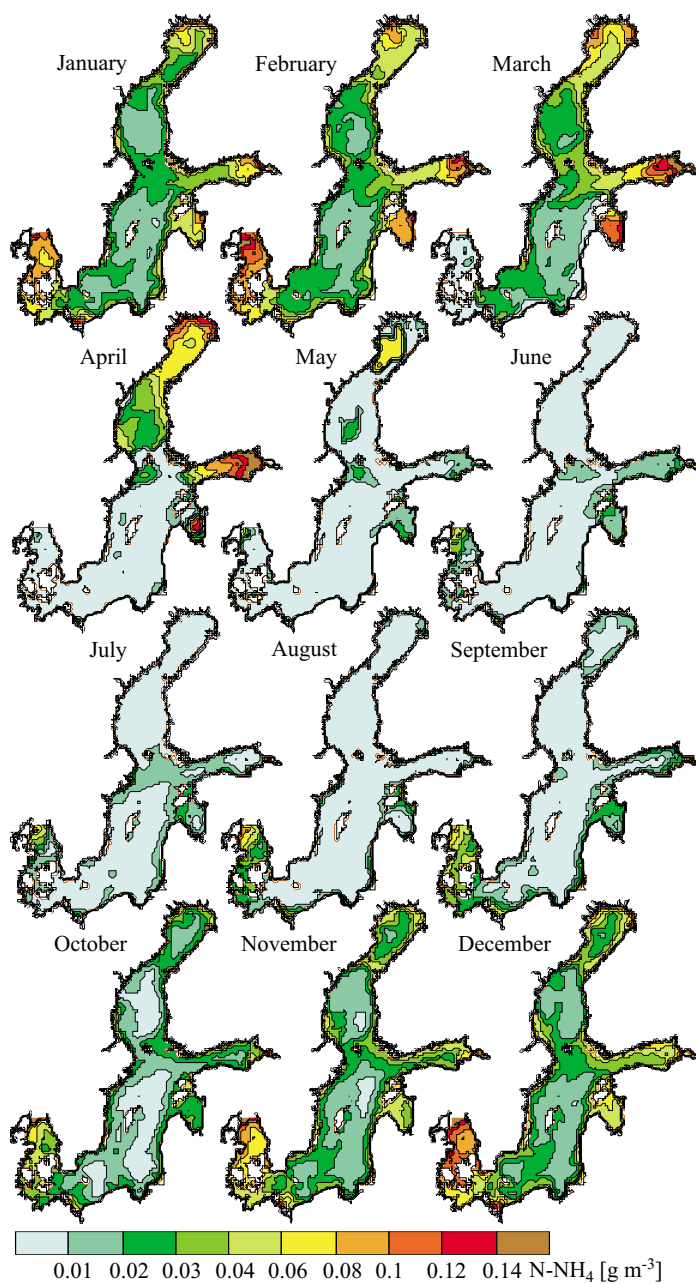


Fig. 11. Surface distribution of ammonium nitrogen for the year 2000

an extended biological part and the parameterisation of water-sediment exchange. The division of phytoplankton into two groups is another development in comparison with previous versions, allowing diatoms and

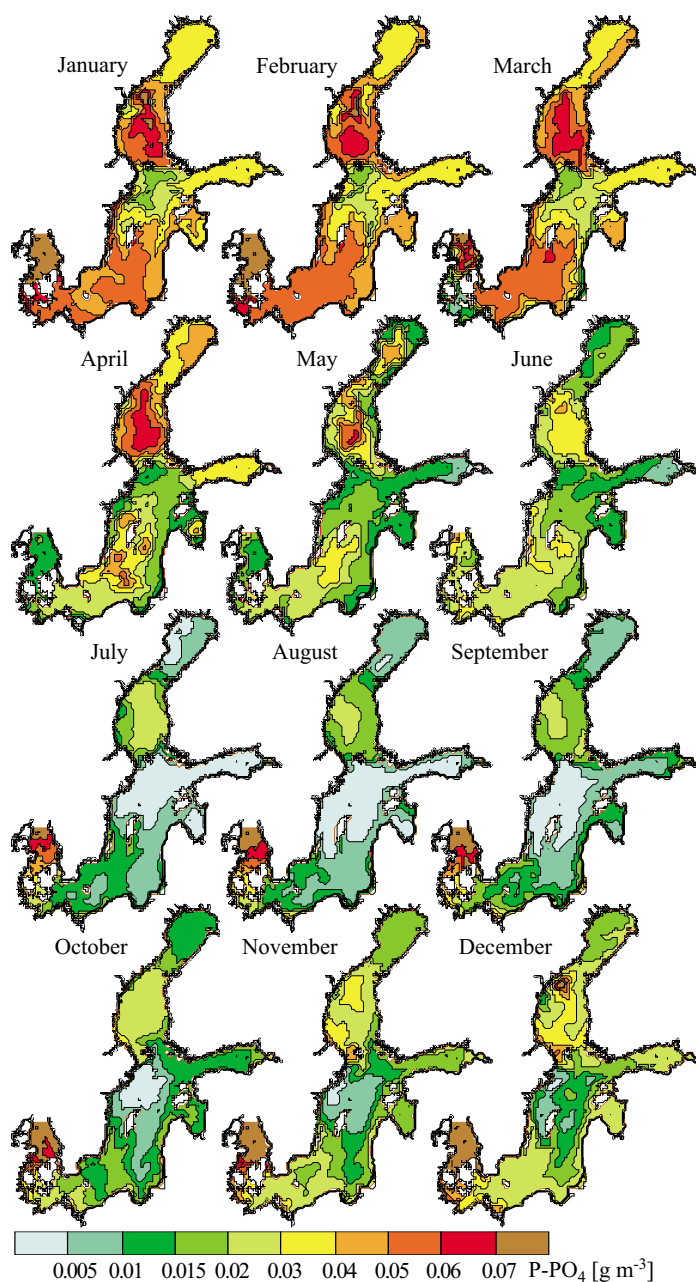


Fig. 12. Surface distribution of phosphate phosphorus for the year 2000

other phytoplankton groups to be analysed separately. Furthermore, it enables the spring diatom bloom and the summer development of phytoplankton to be described, but precludes the mapping of the late-autumn

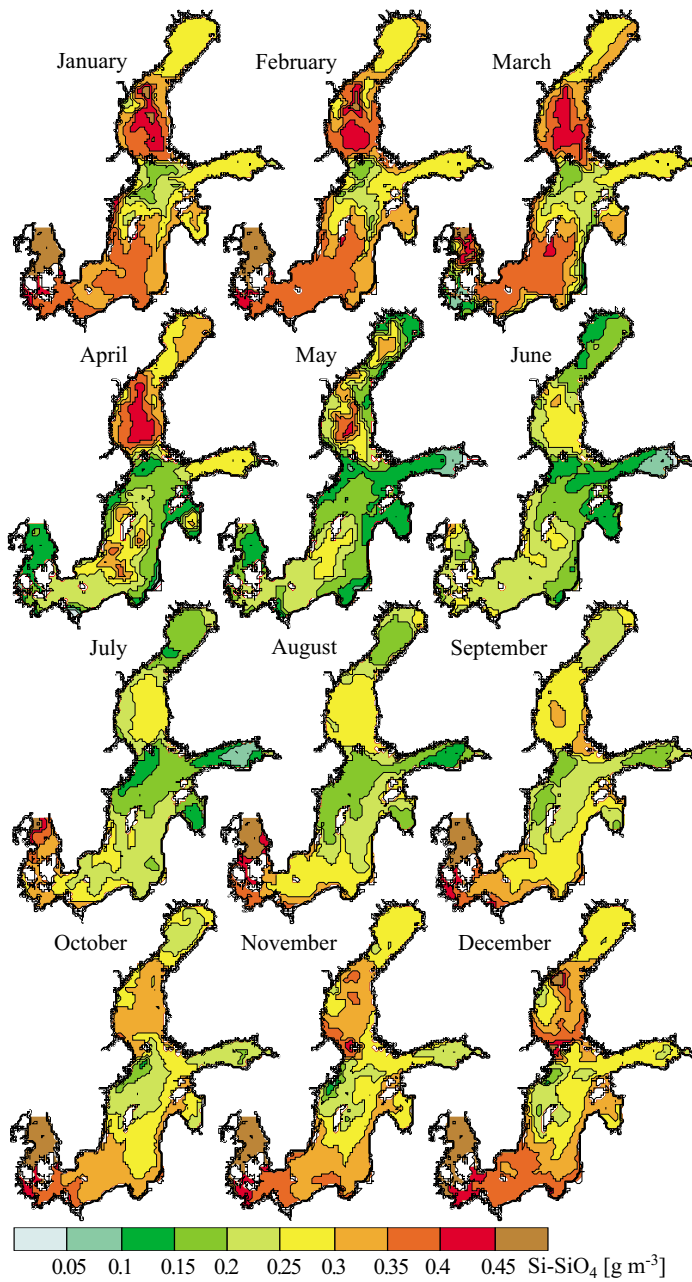


Fig. 13. Surface distribution of silicate silicon for the year 2000

diatom bloom, which in the Gulf of Gdańsk usually takes place in October-November. Witek (1995) claims that at this time the phytoplankton biomass is twice as large as in the summer, when the large diatoms make up

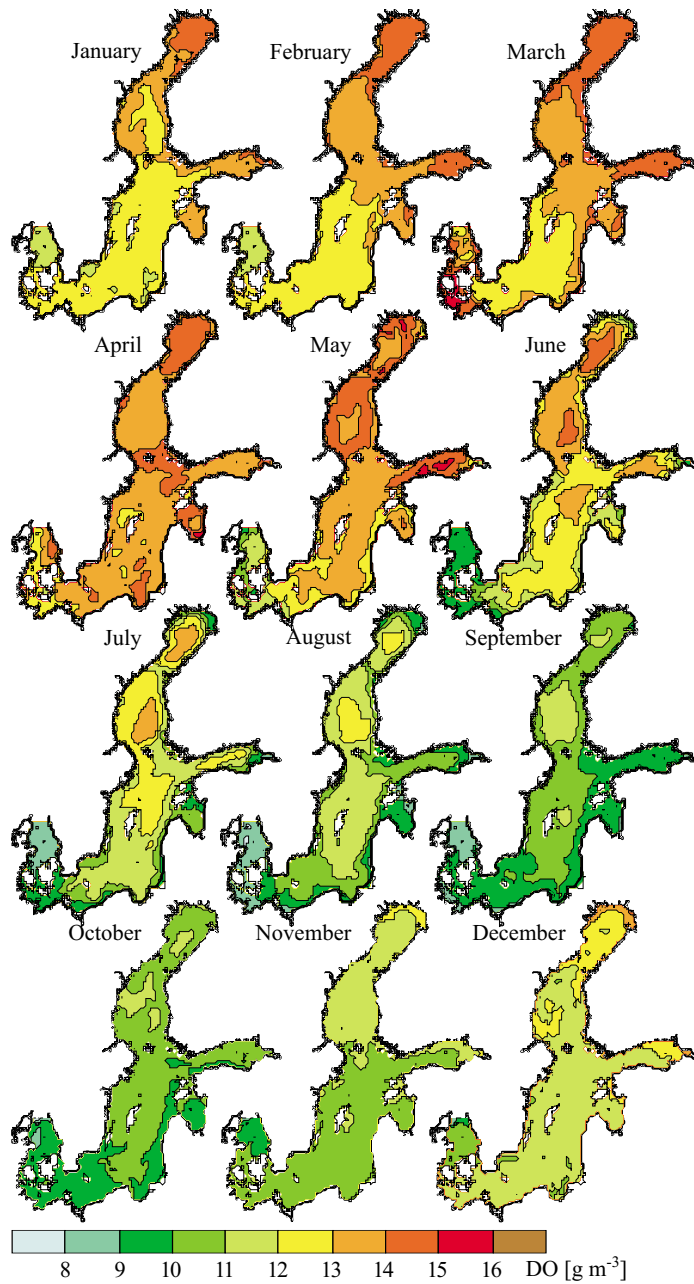


Fig. 14. Surface distribution of dissolved oxygen for the year 2000

the largest percentage of the biomass. Several model examinations show that late-autumn blooms occur, despite the use of only one group of phytoplankton in the model (Ołdakowski & Renk 1997, Savchuk & Wulff 1993).

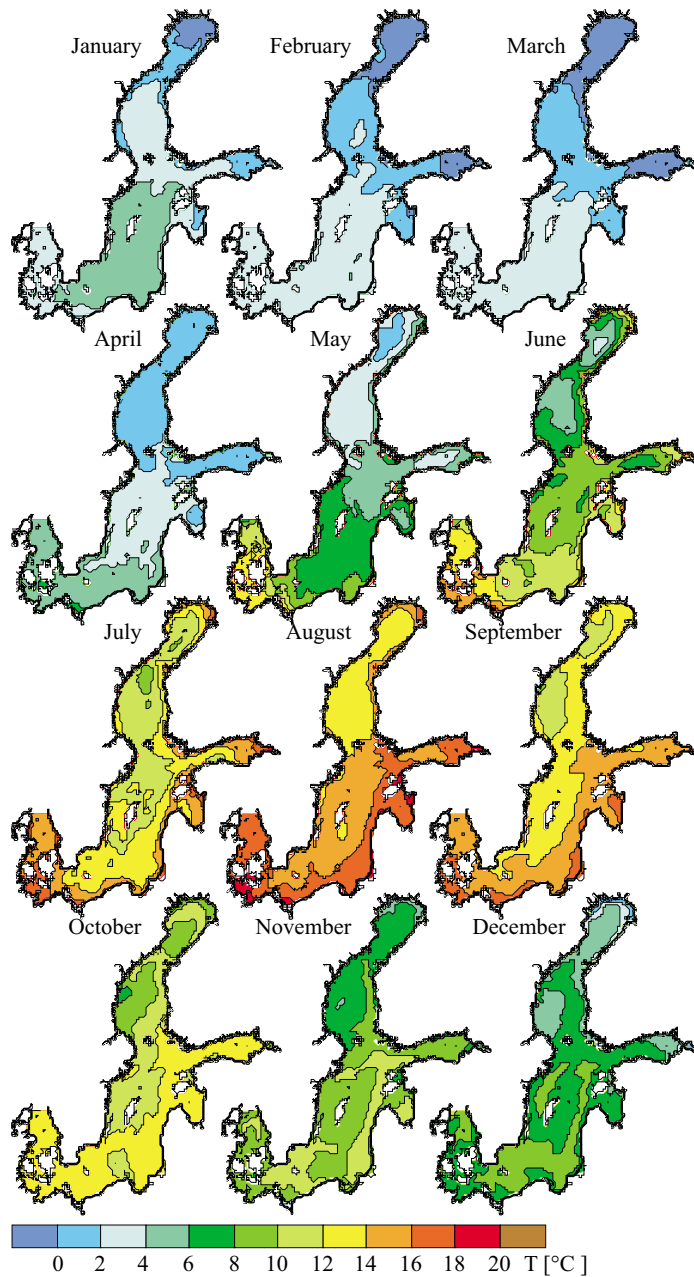


Fig. 15. Surface distribution of water temperature for the year 2000

Two groups of phytoplankton, i.e. diatoms and flagellates were used for researching the North Sea with the ERSEM model (Blackford & Radford 1995, Varela et al. 1995). Neumann (2000) defined the variability of three

phytoplankton groups – diatoms, flagellates and blue-green algae – in his model research, but his results show no autumn diatom bloom either.

For a better description of the seasonal variability in the phytoplankton biomass in the ProDeMo model, we need to consider a larger number of phytoplankton groups: spring diatoms, blue-green algae, autumn diatoms and one group from the summer phytoplankton (green algae, flagellates and dinoflagellates). Each of these groups requires the definition of parameters describing their growth rates, and the parameters of their disappearance from the water (consumption by zooplankton, respiration, decay), which makes the model more complex and difficult to calibrate. The present version of the model does not define blue-green algae as a separate group of phytoplankton. Thus, it does not take into consideration the air-to-water current of nitrogen during the uptake of atmospheric nitrogen by blue-green algae, which comes into being when its mineral forms are lacking in the water. Research has shown (Rahm et al. 2000) that nitrogen assimilation by blue-green algae may be responsible for about 1/5 of the total nitrogen load supplied to the Baltic Proper.

At the present stage of the model's development, considering one zooplankton group appears to be sufficient. On the other hand, more advanced models like the ERSEM envisage a division of the zooplankton into micro- and meso- forms (Baretta-Bekker et al. 1995, Broekhuizen et al. 1995), but this is the consequence of using a more advanced biological module that embraces a higher trophic level.

The approximation of water-sediment exchange applied in the present version of the model enables the changes in nutrient content in the sediment to be simulated on a seasonal basis. Modelling the nutrient fluxes between water and sediment on a larger temporal scale would necessitate changes in the algorithm involving both the variability of the nutrient content in relation to depth and the division of the sediment into oxygenated and anaerobic layers (Ruardij & Van Raaphorts 1995).

The hydrodynamic and ProDeMo models are both resolved on the same horizontal numerical grid, and with the sigma transformation applied in the vertical plane, this allows the same number of layers to be adopted at each point, irrespective of depth. Furthermore, the layers were thinner in shallower waters and thicker in deeper waters. The consequences of using sigma transformations in the hydrodynamic model are well-known (Gary 1973, Haney 1991, Mellor et al. 1994). Much less well understood is the effect of using the same numerical grid for the ecological model calculations. There was a tendency for the steep vertical gradients in the halocline to be smoothed out by the simulations. This is apparent in the vertical distributions of both oxygen and nutrient concentrations and is probably due

to errors arising in the calculations of diffusion done with the aid of the sigma transformation. The separate layers of the numerical grid are not exactly horizontal, which is why a problem arose with the separation of horizontal and vertical diffusion. The turbulent horizontal diffusion coefficients are usually much greater than those of vertical diffusion and so, if the layers of the calculation grid are inclined towards the horizontal, the horizontal diffusion gives rise to an additional component in the vertical direction. This leads to an increase in vertical diffusion, which in consequence causes the smoothing of vertical gradients. To improve the accuracy of the computation of diffusion fluxes, it is sufficient to subtract the climatic mean (Gary 1973, Mellor et al. 1994). Determining a climatic field may be relatively easy with salinity, but is much more difficult with nutrients, owing to their seasonal variability. It seems that the simulated vertical distributions of nutrients and oxygen can be improved through the use of temporally variable climatic fields instead of fixed ones.

In the Kattegatt region, near the model's open boundary, where the exchange of waters between the Baltic and the North Sea takes place, a considerable rise in phosphate and silicate concentrations was observed. This is probably the effect of imperfections in the adopted open boundary condition. The lack of a horizontal gradient in the normal direction towards this border was assumed in the calculations, which implies that the same nutrient concentrations and other state variables occur in the waters flowing in from the Skagerrak and out of the Kattegatt. An improvement in the results of simulations could be achieved by applying boundary conditions to the open border on the basis of measurements conducted in this region.

Furthermore, in order to adequately estimate the nutrient loads entering the Baltic, and to prevent errors, as in the Gulf of Riga, more detailed and suitable input data are needed.

Acknowledgements

We would like to thank the Institute of Meteorology and Water Management, Maritime Branch, in Gdynia for enabling us to access Polish coastal zone monitoring data, which were used for verifying and validating the model. We express our gratitude to Prof. J. Cyberski for preparing the data on the water flow of rivers of the Baltic drainage area. Our thanks also go to Dr S. Gromisz, Prof. L. Falkowska, Dr D. Burska, Prof. Z. Witek, Dr M. Matciak and Dr O. Savchuk for the fruitful discussions and their suggestions for carrying out this work.

References

- Baretta J. W., Admiraal W., Colijn F., Malschaert J. F. P., Ruardij P., 1988, *The construction of the pelagic submodel* [in:] *Tidal flat estuaries: simulation and analysis of the Ems estuary*, J. W. Baretta & P. Ruardij (eds.), Ecol. Stud. 71, Springer-Verl., Berlin, 77–104.
- Baretta J. W., Ebenhöh W., Raurdij P., 1995, *The European Regional Seas Ecosystem Model, a complex marine ecosystem model*, Nether. J. Sea Res., 33 (3)–(4), 223–246.
- Baretta-Bekker J. G., Baretta J. W., Koch Rasmussen E., 1995, *The microbial food web in the European Regional Seas Ecosystem Model*, Nether. J. Sea Res., 33 (3)–(4), 363–379.
- Blackford J. C., Radford P. J., 1995, *A structure and methodology for marine ecosystem modelling*, Nether. J. Sea Res., 33 (3)–(4), 247–260.
- Blumberg A. F., Mellor G. L., 1987, *A description of the three-dimensional coastal ocean circulation model*, pp. 1–16, [in:] *Three-dimensional Coastal Ocean Models*, N. S. Heaps (ed.), Am. Geophys. Union, Washington, 208 pp.
- Broekhuizen N., Heath M. R., Hay S. J., Gurney W. S. C., 1995, *Modelling of dynamics of the North Sea's mesozooplankton*, Nether. J. Sea Res., 33 (3)–(4), 381–406.
- Cyberski J., 1997, *Riverine water outflow into the Gulf of Gdańsk*, Oceanol. Stud., 26 (4), 65–75.
- Delhez E. J. M., 1998, *Macroscale ecohydrodynamic modelling on the Northwest European Continental Shelf*, J. Marine Syst., 16 (1)–(2), 171–190.
- Elken J. (ed.), 1996, *Deep water overflow, circulation and vertical exchange in the Baltic proper*, Est. Mar. Inst. Rep. Ser. No 6 (Tallinn), 91 pp.
- Falkowska L., 1985, *The input of nitrogen and phosphorus compounds from the atmosphere to the Baltic on the basis of investigations in 1981 and 1983*, Stud. Mater. Oceanol., 48, 5–28, (in Polish).
- Fennel K., Losch M., Schröter J., Wenzel M., 2001, *Testing a marine ecosystem model: sensitivity analysis and parameter optimisation*, J. Marine Syst., 28 (1)–(2), 45–63.
- Fennel W., Neumann T., 1996, *The mesoscale variability of nutrients and plankton as seen in a coupled model*, Dt. Hydrogr. Z., 48 (1), 49–71.
- Franz H. G., Mommaerts J. P., Radach G., 1991, *Ecological modelling of the North Sea*, Nether. J. Sea Res., 28 (1)–(2), 67–140.
- Gary J. M., 1973, *Estimate of truncation errors in transformed coordinate, primitive equation atmospheric models*, J. Atmos. Sci., 30, 223–233.
- Gordon D. C. Jr., Boudreau P. R., Mann K. H., Ong J.-E., Silvert W. L., Smith S. V., Wattayakorn G., Wulff F., Yanagi T., 1995, *Biogeochemical modelling guidelines*, LOICZ/R&S/95-5, LOICZ, Texel, The Netherlands, 96 pp.
- Haney R. L., 1991, *On the pressure gradient force over steep topography in sigma coordinate ocean models*, J. Phys. Oceanogr., 21, 610–619.

- Herman-Iżycki L., Jakubiak B., Nowiński K., Niezgódka B., 2002, *UMPL – numerical weather prediction system for operational applications*, [in:] *Research works based on the ICM's UMPL numerical weather prediction system results*, Wyd. Uniw. Warsz., Warszawa, 14–27.
- Hoch T., Garreau P., 1998, *Phytoplankton dynamics in the English Channel: a simplified three-dimensional approach*, *J. Marine Syst.*, 16 (1)–(2), 133–150.
- Jędrasik J., 1997, *A model of matter exchange and flow of energy in the Gulf of Gdańsk ecosystem – overview*, *Oceanol. Stud.*, 26 (4), 3–20.
- Jędrasik J., Szymelfenig M., 2005, *Ecohydrodynamic model of the Baltic Sea. Part 2. Validation of the model*, *Oceanologia*, 47 (4), 543–566.
- Jørgensen S. E., 1998, *Fundamentals of ecological modelling*, Elsevier, Amsterdam, 1–175, 251–314.
- Kowalewski M., 1997, *A three-dimensional, hydrodynamic model of the Gulf of Gdańsk*, *Oceanol. Stud.*, 26 (4), 77–98.
- Kreżel A., 1997, *A model of solar energy input to the sea surface*, *Oceanol. Stud.*, 26 (4), 21–34.
- Marmefelt E., Håkansson B., Erichsen A. Ch., Hansen I. S., 2000, *Development of an ecological model system for the Kattegat and the southern Baltic. Final report to the Nordic Councils of Ministers*, SMHI Rep. Oceanogr. No 29, 76 pp.
- Mellor, G. L., Ezer T., Oey L. Y., 1994, *The pressure gradient conundrum of sigma coordinate ocean models*, *J. Atmos. Ocean. Tech.*, 11 (4), 1126–1134.
- Moll A., 1997, *Phosphate and plankton dynamics during a drift experiment in the German Bight: simulation of phosphorus-related plankton production*, *Mar. Ecol. Prog. Ser.*, 156, 289–297.
- Moll A., 1998, *Regional distribution of primary production in the North Sea simulated by three-dimensional model*, *J. Marine Syst.*, 16 (1)–(2), 151–170.
- Neumann T., 2000, *Towards a 3D-ecosystem model of the Baltic Sea*, *J. Marine Syst.*, 25 (3)–(4), 405–419.
- Oldakowski B., Kowalewski M., Jędrasik J., 1994, *The nutrient dynamic model for the Gulf of Gdańsk*, *Proc. 19th Conf. Baltic Oceanogr.*, Sopot, 528–543.
- Oldakowski B., Renk H., 1997, *The conception and structure of the production-destruction of organic matter model; verification tests for the Gulf of Gdańsk*, *Oceanol. Stud.*, 26 (4), 99–122.
- Radach G., Lenhart H. J., 1995, *Nutrient dynamics in the North Sea: fluxes and budgets in the water column derived from ERSEM*, *Nether. J. Sea Res.*, 33 (3)–(4), 301–335.
- Rahm L., Jönsson A., Wulff F., 2000, *Nitrogen fixation in the Baltic proper: an empirical study*, *J. Marine Syst.*, 25 (3)–(4), 239–248.
- Ruardij P., Van Raaphorst W., 1995, *Benthic nutrient regeneration in the ERSEM ecosystem model of the North Sea*, *Nether. J. Sea Res.*, 33 (3)–(4), 453–483.
- Savchuk O., Wulff F., 1993, *Biogeochemical transformations of nitrogen and phosphorus – a pelagic submodel for the Baltic Sea*, *SMHI Rep. No 1*, 50 pp.

- Savchuk O., Wulff F., 1996, *Biogeochemical transformations of nitrogen and phosphorus in the marine environment – coupling hydrodynamic and biogeochemical processes in models for Baltic Proper*, SMHI Rep. No 2, 79 pp.
- Semovski S.V., Woźniak B., 1995, *Model of the annual phytoplankton cycle in a marine ecosystem – assimilation of monthly satellite chlorophyll data for the North Atlantic and Baltic*, *Oceanologia*, 37 (1), 3–31.
- Semovski S.V., Woźniak B., Hapter R., Staśkiewicz A., 1996, *Gulf of Gdańsk spring bloom physical, bio-optical and biological modelling and contact data assimilation*, *J. Marine Syst.*, 7 (2)–(4), 145–159.
- Stålnacke P., 1996, *Nutrient loads to the Baltic Sea*, Linköping Stud. Arts Sci. No 146, Linköping Univ., Linköping.
- Stigebrandt A., Wulff F., 1987, *A model for the dynamics of nutrients and oxygen in the Baltic proper*, *J. Mar. Res.*, 45, 729–759
- Suursaar Ü., Astok V. (eds.), 1996, *Studies on measuring and modelling of the water and nutrient exchange of the Gulf of Riga*, Est. Mar. Inst. Rep. Ser. No 3 (Tallinn), 109 pp.
- Szymelfenig M. (eds.), 1997, *Modelowanie ekosystemu Zatoki Gdańskiej*, Mater. Konf. Uniw. Gd., Gdańsk.
- Tamsalu R. (ed.), 1996, *Coupled 3D hydrodynamic and ecosystem model FINEST*, Est. Mar. Inst. Rep. Ser. No 15 (Tallinn), 1–113.
- Van der Vat M.P., 1994, *Modelling of eutrophication of the Bay of Gdańsk as a tool for decision makers*, Proc. 19th Conf. Baltic Oceanogr., Sopot, 497–505.
- Varela R.A., Cruzado A., Gabaldón J.E., 1995, *Modelling primary production in the North Sea using the European Regional Seas Ecosystem Model*, *Nether. J. Sea Res.*, 33 (3)–(4), 337–361.
- Vested H.J., Baretta J.W., Ekebjærg L.C., Labrosse A., 1996, *Coupling of hydrodynamical transport and ecological models for 2D horizontal flow*, *J. Marine Syst.*, 8 (3)–(4), 255–267.
- Witek Z., 1995, *Biological production and its consumption in the marine ecosystem of the western Gdańsk Basin*, Wyd. Mor. Inst. Ryb., Gdynia, 145 pp., (in Polish).
- Witek Z., Bralewska J., Chmielewski H., Drgas A., Gostkowska J., Kopacz M., Knurowski J., Krajewska-Soltys J., Lorenz Z., Maciejewska K., Mackiewicz T., Nakonieczny J., Ochocki S., Warzocha J., Piechura J., Renk H., Stopiński M., Witek B., 1993, *Structure and function of marine ecosystem in the Gdańsk Basin on the basis of studies performed in 1987*, *Stud. Mater. Oceanol.*, 63, 5–125.

Appendix 1

Calibration coefficients

Table A1-1. Calibration coefficients for phytoplankton

| Coefficient | Value | | Unit | Description |
|------------------|-------|-------|--------------------|--|
| | DIAT | nDIAT | | |
| G_{\max} | 2.9 | 2.4 | d^{-1} | Maximum growth rate for phytoplankton |
| T_{opt} | 2.0 | 13.0 | $^{\circ}\text{C}$ | Optimum temperature for phytoplankton growth |
| T_{\min} | 0.0 | 5.0 | $^{\circ}\text{C}$ | Minimum temperature for phytoplankton growth |
| T_{\max} | 20.0 | 25.0 | $^{\circ}\text{C}$ | Maximum temperature for phytoplankton growth |
| I_s | 60.0 | 200.0 | W m^{-2} | Optimum light intensity for phytoplankton growth |
| K_{MN} | 0.01 | 0.002 | g m^{-3} | Michelis constant for nitrogen |
| K_{MP} | 0.004 | 0.002 | g m^{-3} | Michelis constant for phosphorus |
| K_{Msi} | 0.03 | 0.0 | g m^{-3} | Michelis constant for silicon |
| K_{Rakt} | 0.0 | 0.0 | – | Parameter for active respiration |
| K_{Rstr} | 0.0 | 0.0 | – | Parameter for stress respiration |
| D_{Rbie} | 0.1 | 0.1 | – | Parameter for non-active respiration |
| Q_{Rbie} | 1.09 | 1.09 | – | Temperature constant for non-active respiration |
| L | 0.05 | 0.05 | d^{-1} | Phytoplankton mortality rate |
| P_{aval} | 0.6 | 1.0 | – | Parameter of food availability |
| V_s | 1.5 | 0.1 | m d^{-1} | Sedimentation rate |
| C_{chl} | 50.0 | 50.0 | – | C-org./chlorophyll <i>a</i> ratio in the phytoplankton biomass |

Table A1-2. Calibration coefficients for zooplankton

| Coefficient | Value | Unit | Description |
|--------------|-------|---|---|
| FrZ_{\max} | 5.00 | $\text{m}^3 \text{gC}^{-1} \text{d}^{-1}$ | Maximum phytoplankton filtration rate |
| Q_Z | 1.07 | – | Temperature constant for zooplankton |
| a_{fr} | 3.00 | – | Filtration constant for zooplankton |
| b_{fr} | 50.00 | $\text{m}^3 \text{g}^{-1}$ | Parameter for filtration by zooplankton |
| Z_{as} | 0.80 | – | Parameter for assimilation by zooplankton |
| K_{Zakt} | 0.02 | – | Parameter for active respiration |
| D_{RbieZ} | 0.02 | – | Parameter for non-active respiration |
| Q_{RbieZ} | 1.07 | – | Temperature constant for non-active respiration |
| L_Z | 0.02 | d^{-1} | Zooplankton mortality rate |

Table A1-3. Calibration coefficients for carbon

| Coefficient | Value | Unit | Description |
|-------------|-------|-----------------|---|
| K_{mC} | 0.03 | d^{-1} | Carbon mineralisation rate |
| Q_{mC} | 1.047 | – | Temperature constant for carbon mineralisation rate |

Table A1-3. (*continued*)

| Coefficient | Value | Unit | Description |
|-------------|-------|-------------------|---|
| M_{DOC} | 1.0 | – | Oxygen parameter for carbon mineralisation rate |
| V_{sDE} | 0.15 | m d^{-1} | Detritus sedimentation rate |
| K_{mCS} | 0.01 | – | Carbon mineralisation rate in sediment |
| Q_{mCS} | 1.0 | – | Temperature constant for carbon mineralisation rate in sediment |
| C_S | 30 | g m^{-2} | Carbon content in sediment |

Table A1-4. Calibration coefficients for nitrogen

| Coefficient | Value | Unit | Description |
|---------------|-------|------------------------------|--|
| K_{nN} | 0.07 | d^{-1} | Nitrification coefficient |
| Q_{nN} | 1.1 | – | Temperature constant for nitrification |
| T_{KrnN} | 2.0 | $^{\circ}\text{C}$ | Critical temperature for nitrification |
| DO_{KrnN} | 3.0 | $\text{gO}_2 \text{ m}^{-3}$ | Critical oxygen content for nitrification |
| K_{dnN} | 0.09 | d^{-1} | Denitrification coefficient |
| Q_{dnN} | 1.12 | – | Temperature constant for denitrification |
| T_{KrdnN} | 2.0 | $^{\circ}\text{C}$ | Critical temperature for denitrification |
| DO_{MaxdnN} | 2.0 | $\text{gO}_2 \text{ m}^{-3}$ | Critical oxygen (maximum) content for denitrification |
| DO_{KrdnN} | 0.5 | $\text{gO}_2 \text{ m}^{-3}$ | Critical oxygen content for denitrification |
| K_{rdnN} | 4.0 | – | Multiplication factor for denitrification below the critical value of the oxygen content |
| K_{mN} | 0.005 | d^{-1} | Nitrogen mineralisation rate |
| Q_{mN} | 1.1 | – | Temperature constant for nitrogen mineralisation |
| M_{DON} | 1.0 | – | Oxygen parameter for nitrogen mineralisation |
| a_{NCD} | 0.22 | – | Carbon to nitrogen ratio for diatoms |
| a_{NCnD} | 0.22 | – | Carbon to nitrogen ratio for non-diatoms |
| a_{NCD} | 0.07 | – | Carbon to nitrogen ratio for zooplankton |
| K_{mNS} | 0.005 | – | Nitrogen mineralisation rate in sediment |
| Q_{mNS} | 1.0 | – | Temperature constant for nitrogen mineralisation in sediment |
| F_{Snitr} | 0.0 | – | Fraction of ammonium nitrogen undergoing immediate nitrification in sediment |
| F_{Sden} | 0.7 | – | Fraction of nitrate nitrogen undergoing immediate denitrification in sediment |

Table A1-5. Calibration coefficients for phosphorus

| Coefficient | Value | Unit | Description |
|-------------|-------|-----------------|--|
| K_{mP} | 0.01 | d^{-1} | Phosphorus mineralisation rate |
| Q_{mP} | 1.047 | – | Temperature constant for phosphorus mineralisation |
| M_{DOP} | 1.0 | – | Oxygen parameter for phosphorus mineralisation |

Table A1-5. (*continued*)

| Coefficient | Value | Unit | Description |
|-------------|-------|-------------------|--|
| a_{PCD} | 0.025 | – | Carbon to phosphorus ratio for diatoms |
| a_{PCnD} | 0.025 | – | Carbon to phosphorus ratio for non-diatoms |
| a_{PCD} | 0.002 | – | Carbon to phosphorus ratio for zooplankton |
| F_{pip} | 0.3 | – | Fraction of phosphorus adsorbed on inorganic particles |
| V_{sSP} | 0.35 | m d^{-1} | Sedimentation rate of inorganic particles |
| K_{mPS} | 0.01 | – | Phosphorus mineralisation rate in sediment |
| Q_{mPS} | 1.0 | – | Temperature constant for phosphorus mineralisation in sediment |

Table A1-6. Calibration coefficients for silicon

| Coefficient | Value | Unit | Description |
|-------------|-------|-----------------|---|
| K_{mSi} | 0.005 | d^{-1} | Silicon mineralisation rate |
| Q_{mSi} | 1.047 | – | Temperature constant for silicon mineralisation |
| M_{DOSi} | 1.0 | – | Oxygen parameter for silicon mineralisation |
| a_{SiCD} | 0.2 | – | Carbon to silicon ratio for diatoms |
| a_{SiCD} | 0.0 | – | Carbon to silicon ratio for zooplankton |
| K_{mSiS} | 0.015 | – | Silicon mineralisation rate in sediment |
| Q_{mSiS} | 1.0 | – | Temperature constant for silicon mineralisation in sediment |

Table A1-7. Calibration coefficients for oxygen

| Coefficient | Value | Unit | Description |
|-------------|-------|--|---|
| B_{DO} | 0.3 | $\text{m}^1 \text{d}^{-1}$ | Parameter for oxygen flux to atmosphere under oversaturation conditions |
| R_{DOW} | 0.2 | $\text{s}^2 \text{m}^{-1} \text{d}^{-1}$ | Re-aeration coefficient |
| a_{OC} | 2.67 | – | Oxygen to carbon ratio during photosynthesis |
| a_{Onn} | 5.71 | – | Oxygen to nitrogen ratio during nitrification |
| a_{Onden} | 3.43 | – | Oxygen to nitrogen ratio during denitrification |
| a_{Omm} | 2.06 | – | Oxygen to nitrogen ratio during mineralisation |
| a_{Opm} | 2.06 | – | Oxygen to phosphorus ratio during mineralisation |
| a_{Osim} | 2.29 | – | Oxygen to silicon ratio during mineralisation |

Table A1-8. Parameters for light penetration

| Parameter | Value | Unit | Description |
|--------------|-------|----------------------------|--|
| Kd_0 | 0.17 | m^{-1} | Light extinction coefficient (steady value) |
| $Kd_{Chl a}$ | 25.0 | $\text{m}^2 \text{g}^{-1}$ | Light extinction coefficient depending on chlorophyll concentration |
| Kd_{OC} | 0.0 | $\text{m}^2 \text{g}^{-1}$ | Light extinction coefficient depending on organic carbon concentration |

Appendix 2

ProDeMo equations

A2.1 Phytoplankton

Change in phytoplankton mass:

$$\frac{\partial [C_i]}{\partial t} = (G_i - R_i - D_{Zi} - L_i) [C_i] + V_{S_i} \frac{\partial [C_i]}{\partial z},$$

where

G_i – phytoplankton growth;

R_i – phytoplankton respiration;

D_{Z_i} – grazing of phytoplankton;

L_i – decay of phytoplankton;

i – phytoplankton group (DIAT or nDIAT).

Phytoplankton growth (G_i):

$$G_i = G_{\max_i} G_{T_i} G_{I_i} G_{B_i}.$$

Phytoplankton growth as a function of water temperature:

$$G_{T_i} = \exp \left\{ \begin{array}{ll} 2.3 \left(\frac{T - T_{opt_i}}{T_{opt_i} - T_{min_i}} \right)^2 & T \leq T_{opt_i} \\ 2.3 \left(\frac{T - T_{opt_i}}{T_{max_i} - T_{opt_i}} \right)^2 & T > T_{opt_i} \end{array} \right\}.$$

Phytoplankton growth in relation to the intensity of active radiation – I_{PAR} [W m^{-2}]:

$$G_{I_i} = \frac{I_{PAR}}{I_{S_i}} \exp \left[1 - \frac{I_{PAR}}{I_{S_i}} \right].$$

The value of I_{PAR} at a given depth is determined by solving the equation:

$$\frac{\partial I_{PAR}}{\partial z} = I_{PAR} \left(Kd_0 + Kd_{Chl a} \sum_i [C_i] C_{Chl_i} + Kd_{OC} [C_{DETR}] \right).$$

Phytoplankton growth in relation to the concentration of nutrients:

$$G_{B_i} = \min(G_{N_i}, G_{P_i}, G_{Si_i}).$$

Phytoplankton growth depending on the concentration of inorganic nitrogen:

$$G_{N_i} = \frac{[N-NH_4] + [N-NO_3]}{K_{MN_i} + ([N-NH_4] + [N-NO_3])}.$$

Phytoplankton growth depending on the concentration of inorganic phosphorus:

$$G_{P_i} = \frac{[P-PO_4]}{K_{MP_i} + [P-PO_4]}.$$

Phytoplankton growth depending on the concentration of inorganic silicon:

$$G_{Si_i} = \frac{[Si-SiO_4]}{K_{MSi_i} + [Si-SiO_4]}.$$

Respiration of phytoplankton (R_i):

$$R_i = K_{Rakt_i} G_i + K_{Rstr_i} G_i \left(1 - \frac{1}{G_{B_i}} \right) + D_{Rbie_i} Q_{Rbie_i}^{T-20}.$$

Grazing of phytoplankton by zooplankton (D_{Zi}):

$$D_{Zi} = P_{aval_i} Fr [C_{ZOO}].$$

Filtration by zooplankton:

$$Fr = \frac{Fr_{Zmax} Q_Z^{T-20}}{1 + \exp\left(a_{fr} - b_{fr} \sum_i P_{aval_i} [C_i]\right)}.$$

A2.2 Zooplankton

Change in zooplankton biomass:

$$\frac{\partial [C_{ZOO}]}{\partial t} = (A_Z - R_Z - L_Z) [C_{ZOO}],$$

where

A_Z – assimilation of phytoplankton by zooplankton;

R_Z – zooplankton respiration;

L_Z – decay of zooplankton.

Assimilation of phytoplankton by zooplankton:

$$A_Z = Z_{As} Fr \sum_i P_{aval_i} [C_i].$$

Zooplankton respiration (R_Z):

$$R_Z = K_{Zakt} A_Z + D_{RbieZ} Q_{RbieZ}^{T-20}.$$

Excretion by zooplankton [d^{-1}]:

$$L_Z = Fr \sum_i P_{aval_i} [C_i] - A_Z.$$

A2.3 Mineralisation of carbon, nitrogen, phosphorus and silicon

Coefficient of mineralisation of carbon, nitrogen, phosphorus and silicon depending on the temperature and concentration of oxygen (M_C , M_N , M_P , M_{Si} , M_{CS} , M_{NS} , M_{PS} , M_{SiS}):

$$M_X = K_{mX} Q_{mX}^{T-20} \frac{[DO]^2}{M_{DOX} + [DO]^2}$$

where

X – carbon (C), carbon in sediment (C_S), nitrogen (N), nitrogen in sediment (N_{SED}), phosphorus (P), phosphorus in sediment (P_{SED}), silicon (Si) or silicon in sediment (Si_{SED});

M_{DOX} – oxygen coefficient of mineralisation.

A2.4 Carbon in detritus

$$\begin{aligned} \frac{\partial [C_{DETR}]}{\partial t} &= \\ &= \sum_i L_i [C_i] + (L_Z + W_Z) [C_{ZOO}] - M_C [C_{DETR}] + V_{sDETR} \frac{\partial [C_{DETR}]}{\partial z}. \end{aligned}$$

A2.5 Nitrogen

Fluxes from sediment.

Total flux of inorganic nitrogen (as a result of mineralisation) from sediment to water [$\text{gm}^{-2} \text{d}^{-1}$]:

$$S_N = M_{N_{SED}} [N_{SED}].$$

Fluxes of ammonium nitrogen, nitrate nitrogen from sediment to water [$\text{gm}^{-2} \text{d}^{-1}$]:

$$S_{NH_4} = (1 - F_{SNitr}) S_N, \quad S_{NO_3} = F_{SNitr} (1 - F_{SDen}) S_N.$$

Nitrogen in sediment:

$$\frac{\partial [N_{SED}]}{\partial t} = \sum_i V s_i [C_i] a_{NC_i} + V_{SDE} [N_{DETR}] - S_N.$$

Nitrate nitrogen:

$$\begin{aligned} \frac{\partial [N-NO_3]}{\partial t} &= K_{nN} Q_{nN}^{T-20} [N-NH_4] - K_{dnN} Q_{dnN}^{T-20} [N-NO_3] + \\ &- \sum_i [G_i [C_i] a_{NC_i} (1 - P_{N_i})] + (S_{NO_3} / \Delta z_H)^*, \end{aligned}$$

where

(*) - the last term of the equation applies only to the bottom layer;

Δz_H - thickness of the bottom layer and the phytoplankton group (DIAT, nDIAT).

Preference of ammonium nitrogen uptake over nitrate nitrogen uptake for particular phytoplankton groups:

$$\begin{aligned} P_{N_i} &= \frac{[N-NH_4] [N-NO_3]}{(K_{MN_i} + [N-NH_4]) (K_{MN_i} + [N-NO_3])} + \\ &+ \frac{[N-NH_4] K_{MN_i}}{([N-NH_4] + [N-NO_3]) (K_{MN_i} + [N-NO_3])}. \end{aligned}$$

Ammonium nitrogen:

$$\begin{aligned} \frac{\partial [N-NH_4]}{\partial t} &= M_N [N_{DETR}] + \sum_i (R_i - G_i P_{N_i}) [C_i] a_{NC_i} + \\ &+ R_Z [C_{ZOOPT}] a_{NC_Z} - K_{nN} Q_{nN}^{T-20} [N-NH_4] + (S_{NH_4} \Delta z_H)^*. \end{aligned}$$

Nitrogen in detritus:

$$\begin{aligned} \frac{\partial [N_{DETR}]}{\partial t} &= \sum_i L_i [C_i] a_{NC_i} + (L_Z a_{NC_Z} + W_N) [C_{ZOOPT}] = \\ &- M_N [N_{DETR}] + V_{SDE} \frac{\partial [N_{DETR}]}{\partial z}. \end{aligned}$$

Excretion of nitrogen by zooplankton [d^{-1}]:

$$W_N = Fr \sum_i P_{aval_i} a_{NC_i} [C_i] - A_Z a_{NC_Z}.$$

A2.6 Phosphorus

Fluxes from sediment:

$$S_P = M_{P_{SED}} [P_{SED}].$$

Phosphorus in sediment:

$$\frac{\partial [\text{P}_{\text{SED}}]}{\partial t} = \sum_i V_{s_i} [C_i] a_{PC_i} + V_{s_{DE}} [\text{P}_{\text{DETR}}] - S_P.$$

Phosphate phosphorus:

$$\begin{aligned} \frac{\partial [\text{P-PO}_4]}{\partial t} &= M_P [\text{P}_{\text{DETR}}] + \sum_i (R_i - G_i) [C_i] a_{NC_i} + R_Z [\text{C}_{\text{ZOO}}] a_{PC_Z} + \\ &+ V_{SSP} f_{PIP} \frac{\partial [\text{P-PO}_4]}{\partial z} + (S_P / \Delta z_H)^*. \end{aligned}$$

Phosphorus in detritus:

$$\begin{aligned} \frac{\partial [\text{P}_{\text{DETR}}]}{\partial t} &= \sum_i L_i [C_i] a_{PC_i} + (L_Z a_{PC_Z} + W_P) [\text{C}_{\text{ZOO}}] - M_P [\text{P}_{\text{DETR}}] + \\ &+ V_{s_{DE}} \frac{\partial [\text{P}_{\text{DETR}}]}{\partial z}. \end{aligned}$$

Excretion of phosphorus by zooplankton [d^{-1}]:

$$W_P = Fr \sum_i P_{aval_i} a_{PC_i} [C_i] - A_Z a_{PC_Z}.$$

A2.7 Silicon

Fluxes from sediment:

$$S_{Si} = M_{Si_{SED}} [\text{Si}_{\text{SED}}].$$

Silicon in sediment:

$$\frac{\partial [\text{Si}_{\text{SED}}]}{\partial t} = \sum_i V_{s_i} [C_i] a_{PSi_i} + V_{s_{DE}} [\text{Si}_{\text{DETR}}] - S_{Si}.$$

Silicate silicon:

$$\begin{aligned} \frac{\partial [\text{Si-SiO}_4]}{\partial t} &= M_{Si} [\text{Si}_{\text{DETR}}] + \sum_i (R_i - G_i) [C_i] a_{SiC_i} + R_Z [\text{C}_{\text{ZOO}}] a_{SiC_Z} + \\ &+ (S_{Si} / \Delta z_H)^*. \end{aligned}$$

Silicon in detritus:

$$\begin{aligned} \frac{\partial [\text{Si}_{\text{DETR}}]}{\partial t} &= \sum_i L_i [C_i] a_{SiC_i} + (L_Z a_{SiC_Z} + W_P) [\text{C}_{\text{ZOO}}] - M_{Si} [\text{Si}_{\text{DETR}}] + \\ &+ V_{s_{DE}} \frac{\partial [\text{Si}_{\text{DETR}}]}{\partial z}. \end{aligned}$$

Rate of excretion of silicon by zooplankton [d^{-1}]:

$$W_{Si} = Fr \sum_i P_{aval_i} a_{SiC_i} [C_i] - A_Z a_{SiC_Z}.$$

A2.8 Dissolved oxygen

$$\begin{aligned}
\frac{\partial [\text{DO}]}{\partial t} &= \frac{R_{DO}}{\Delta z} + \\
&+ \left[\sum_i (G_i - R_i) [C_i] - R_Z [\text{C}_{Z\text{OOP}}] - M_C [\text{C}_{\text{DETR}}] - (S_C / \Delta z)^* \right] a_{OC} + \\
&+ \left[- \sum_i R_i [C_i] a_{PC_i} - R_Z a_{PC_Z} [\text{C}_{Z\text{OOP}}] - M_P [\text{P}_{\text{DETR}}] - (S_P / \Delta z)^* \right] a_{OP} + \\
&+ \left[- \sum_i R_i [C_i] a_{SiC_i} - R_Z a_{SiC_Z} [\text{C}_{Z\text{OOP}}] - M_{Si} [\text{Si}_{\text{DETR}}] - (S_{Si} / \Delta z)^* \right] a_{OSi} + \\
&+ K_{dnN} Q_{dnN}^{T-20} [\text{N-NO}_3] a_{ON_{dn}} - \left[K_{nN} Q_{nN}^{T-20} [\text{N-NH}_4] + (S_{NO_3} \Delta z)^* \right] a_{ON_n}.
\end{aligned}$$

Oxygenation as a result of re-aeration or removal of extra oxygen in the case of oversaturation:

$$R_{DO} = \begin{cases} (R_{DO_w} U_{10}^2 (C_{ST} - [\text{DO}]))^{**} & \text{when } [\text{DO}] \leq C_{ST} \\ B_{DO} (C_{ST} - [\text{DO}]) & \text{when } [\text{DO}] > C_{ST}. \end{cases}$$

() ** only for surface layer

Degree of saturation of water with oxygen at a given salinity and temperature:

$$\begin{aligned}
C_{ST} &= 14.652 - S \times 0.0841 + T [S \times 0.00256 - 0.41022 + \\
&+ T (0.007991 - S \times 0.0000374 - T \times 0.000077774)].
\end{aligned}$$